5

CHIRAL POLYMERS WITH PHOTOAFFECTED PHASE BEHAVIOR FOR OPTICAL DATA STORAGE

MIKHAIL V. KOZLOVSKY*,†
LEV M. BLINOV†
WOLFGANG HAASE*
**Institute of Physical Chemistry, Darmstadt University of Technology, Darmstadt, Germany*
†Institute of Crystallography, Russian Academy of Sciences, Moscow, Russia

5.1 INTRODUCTION

During the decade of the 1990s, substantial interest has grown in photoaddressed polymer materials. These systems are characterized by their capability of reversible reorientation and/or photochemical transformations under the action of UV or visible light, followed by corresponding change in such optical properties as birefringence, transparency, or color. Therefore, they are widely investigated as optical data storage and photorecording media, coatings for contactless surface controlling, NLO active materials, and so on.[1,2,3]

Among these photosensitive polymer materials, foremost are the systems containing dichroic azobenzene moieties either as low molar mass components or as fragments of the macromolecule itself. The key physical process involved is the repetitive ***E***/***Z***-isomerization of azobenzene groups, as shown next.

Photoreactive Organic Thin Films

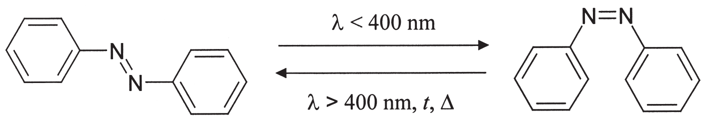

***E*-form (or *trans*-isomer)** **Z-form (or *cis*-isomer)**

In this process, the *trans*-to-*cis* transformation is induced by UV light illumination, whereas the backward conversion at ambient temperature occurs spontaneously but can be accelerated by increasing the temperature or by illumination with yellow light.

The ***E*/*Z***-isomerization process is characterized by angular-dependent excitation and leads, therefore, to the photoselection of a preferred azobezene dye orientation. In other words, the dichroic dye units choose an orientation where the electronic transition moment is perpendicular to the light electric vector. It promotes, in turn, the cooperative reorientation of neighboring moieties, which include other fragments of the macromolecule, such as the main chain or photochemically inactive comonomer units, and low molar mass additives. Thus, a macroscopic orientation of the sample arises, and it remains long after the illumination is stopped and all the dye moieties return to the thermodynamically equilibratory ***E***-state.

To date, various possibilities for incorporating an azobenzene dye into a polymer system have been suggested and tested. First, solid dispersions of low molar mass azo dyes in amorphous polymers were studied.[4–8] Then, the amorphous copolymers containing chemically bound azobenzene fragments were thoroughly investigated.[9–16] Many attempts at combining the photochromism of azobenzene systems with liquid crystallinity have also been performed, probably because of the prominent role of liquid crystals in modern display technology. In the simplest way, azobenzene dye can be dissolved in an LC polymer matrix.[17–19] In addition, with polymer-stabilized liquid crystals (PSLCs), one can introduce orientation into a low molar mass liquid crystal through azobenzene-containing polymer networks,[20,21] while other authors, in an opposite manner, use LC polymer networks and low molar mass azo dyes.[22,23] Optical and electro-optical switching in polymer-dispersed liquid crystals (PDLCs) with azobenzene molecules has been reported as well.[24,25] It is worth noting as well of that Wu *et al.* have performed systematic studies on contactless photoalignment of liquid crystals by thin surface layers of azodye polymers.[26–28]

The most intensively developed materials, however, are the azobenzene-containing side chain LC polymers, which show a unique combination of liquid crystallinity and photochromic behavior in a single macromolecule, whereas copolymerization of comonomers with different functionality allows fine tuning of phase behavior, photo-optical properties, and other parameters to the requirements of a particular application. Starting from the first publications of Eich *et al.*,[29–32] work in that area has been done by several research groups.[33–42] As compared with amorphous polymers, the liquid crystalline systems possess an initial preorientation, which should be overcome during the photo-orientation process. Generally, the higher the degree of mesogenic group ordering, the lower the values of the photoinduced birefringence, because the orientational order in the LC state restricts the reorientation of the mesogenic side chains. That disadvantage can be easily overridden, however, by preliminary misalignment of the LC order using irradiation with non-polarized or circularly polarized UV light. On the other hand, higher ordering of the mesogenic and dye groups in the mesophase leads to higher glass temperatures and, potentially, to enhanced stability of the recorded data or images. Moreover, the competition between the thermodynamic equilibrium LC structure and the photo-optically induced one might result in a number of advanced and sophisticated photorecording techniques, as we will show later in this chapter.

There have also been reports on the preparation of polar materials by a photo-electro-poling technique that combines the optically induced quadrupolar depletion of chromophores in the direction of the light electric vector with an additional field-induced orientation of dipolar chromophores.[43–45] The latter allows the preparation of "cold electrets," which are interesting for non-linear optical applications, such as optical harmonic generation, wave mixing, etc.[3]

Among the known LC phases used for photoaddressed polymer applications, chiral systems attract particular interest due to such features as selective reflection of light, circular polarization of the propagating/reflected light, and ferroelectricity. Thus, for example, Bobrovsky *et al.* have reported recently on the controlled change of a helical pitch and, hence, of a color of cholesteric photochromic copolymers,[46] and dual photoaddressing using light of different wavelengths in terpolymers containing both azobenzene and benzylidene-*p*-menthanone photochromic moieties.[47] Moreover, the photo-induced chromophore reorientation was shown to unwind totally the helical structure of cholesteric oligomers and polymers.[48]

We should note here that most of the publications consider the photo-orientation process and the birefringence it introduces to be the only effect of the light illumination onto dichroic LC polymers. Nevertheless, the elongated ***E***-form and the bent ***Z***-form of the same azo dye molecule generally should reveal quite different phase behaviors: The former favors formation of LC phases, but the latter can hardly accommodate to the mesophase. Hence, the illumination should affect substantially mesophase properties and phase transitions of dichroic LC polymers. Eich, Wendorff, Reck and Ringsdoff's early paper[29] discusses a large shift—up to 10 K—of the clearing point in a nematic azo dye copolymer under illumination. It is no surprise, therefore, that the UV illumination within the temperature gap between the clearing points of completely-*trans* and completely-*cis* isomers, i.e., isotropization temperatures in darkness and under illumination, causes the (isothermal) clearing transition, as reported by Hayashi *et al.*[49] for a high-ordered smectic phase of an azo dye polyacrylate. In that case, the temperature variation of the photo-induced phase transition does not exceed 6 K. However, Ikeda *et al.*[50] report an isothermal photoinduced N-Iso phase transition of photochromic side chain poly(meth)acrylates within a much broader temperature range (from 130°C down to the room temperature), including the region below T_g. The backward transition to the nematic state occurs thermally in darkness, taking some seconds close to the clearing point but much longer at lower temperatures, with an activation energy of about 105 kJ/mol. That I–N transition can be accelerated, however, by illumination with visible light ($\lambda > 420$ nm), *cis*-to-*trans* transformation being the rate-determining step of the transition process. According to Ikeda *et al*,[50] the presence of electron-donating and -accepting groups in *p*,*p′*-positions of the azobenzene core increases the rate of the I–N transition, thus shortening the response time (good for switching applications) but reducing the stability (a disadvantage for photorecording applications).

It should be also mentioned that the conventional appearance of liquid crystals as a polydomain texture results in remarkable light scattering by the domain boundaries. Special efforts should be taken to produce large transparent (monodomain) samples of LC polymers, including shear flow, film stretching, thermal training, external electric or magnetic fields, etc. Such orientation procedures show poor reproducibility, however; they require time and sophisticated equipment. For that reason, it is usual that only thin films of azo dye LC polymers, in which the scattering can be neglected, are investigated as photochromic polymer materials. Among those are Longmuir-Blodgett films consisting of several molecular layers,[38–42,53–55] 0.05 to 0.5-µm-thick spin-coated films,[56–58] and 1 to 5-µm-thick cast films.[26–28,59]

For all these reasons, our recent discovery of chiral side chain polymers, which appear visually amorphous and optically isotropic but possess some hidden LC ordering, is of particular interest. The structure of that “isotropic smectic” (IsoSm*) phase is not completely determined yet; nevertheless, it was successfully used for the creation of novel azo dye copolymer materials that combine spontaneous transparency with mesomorphic (micro)structure, which incorporates photosensitive moieties. In the next section, we consider the structure and properties of the IsoSm* phase of chiral dichroic copolymers and discuss its application to two types of photorecording. One is related to the photoinduced birefringence in polymer films (holographic grating recording), whereas the other is based on the possibility of governing mesomorphic phase transitions in such polymers by light illumination (the light-controlled phase transition—LCPT—recording). Also, we will report an application of such films for contactless orientation of conventional (nematic) liquid crystals.

5.2 AMORPHOUS, OPTICALLY ISOTROPIC MESOPHASE OF CHIRAL SIDE-CHAIN POLYMERS WITH A HIDDEN LAYER STRUCTURE—THE “ISOTROPIC SMECTIC” PHASE

In 1991, Bata *et al.* reported an unusual phase behavior of a chiral side chain polymethacrylate, P8*M.[60]

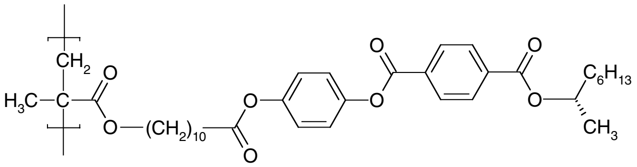

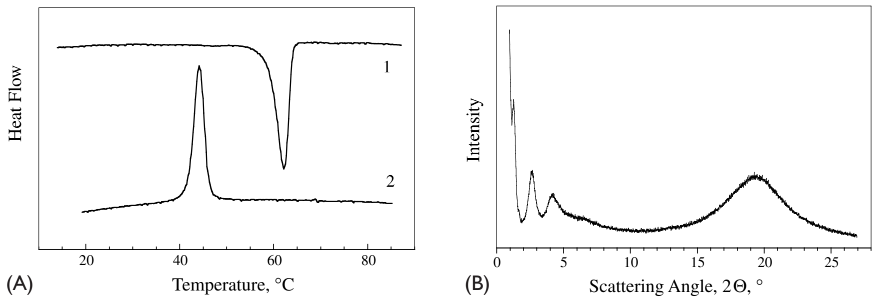

FIG. 5.1 Structural data for P8*M: (A) DSC traces on heating (*1*) and cooling (2); (B) X ray scattering profile below the phase transition (40°C).

This showed a single-phase transition with remarkable hysteresis: at 64°C on heating but at 44°C on cooling. The transition was detected by various experimental techniques including DSC, (see Figure 5.1A), X ray, and broadline NMR.[60,61]

As seen in Figure 5.1B, the polymer forms a layered structure below the transition point, showing a well developed system of SAXS peaks. Moreover, the ORD measurements (see Figure 5.2) exhibit drastic growth of the optic rotation in the IsoSm* phase towards shorter wavelengths, in contrast to the proper isotropic melt of the same polymer above the transition point, suggesting some helix-like superstructural ordering in the mesophase with a pitch below 300 nm.[62] That hypothesis was further supported with CD, dielectric spectroscopy, and UV-vis spectroscopy data.[63,64] The critical importance of chirality for the formation of the IsoSm* phase is also confirmed by

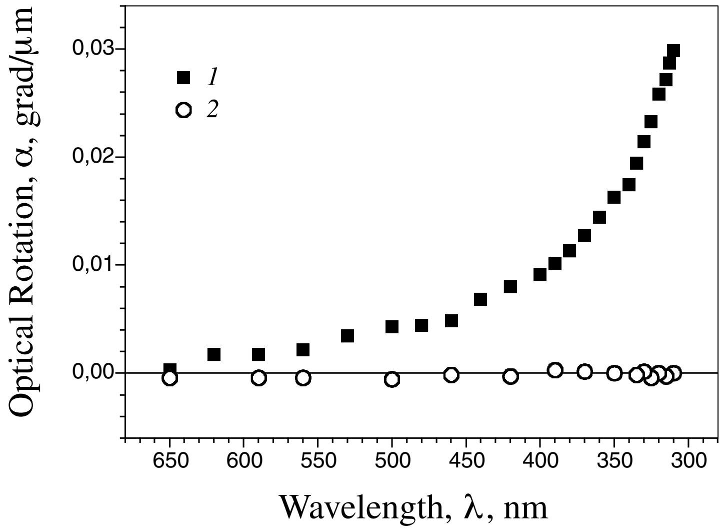

FIG. 5.2 ORD data from P8*M (an 18-μm film) below the phase transition at (*1*) 20°C and above the phase transition at (2) 80°C.

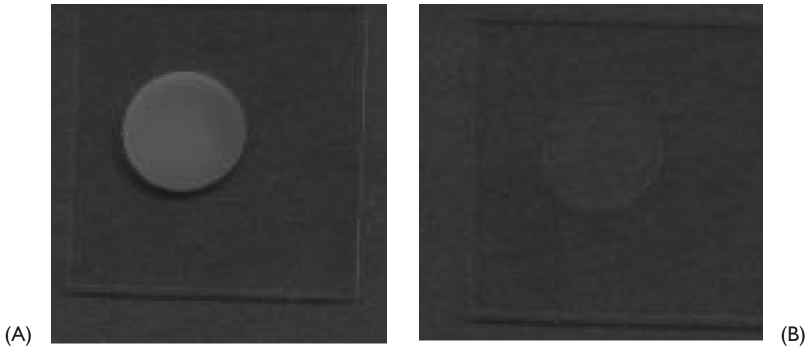

FIG. 5.3 Optical appearance of polymer films: (A) racemic polymer, P8$^{\pm}$M; (B) chiral polymer, P8*M.

the fact that the racemic isomer, P8$^{\pm}$M, forms only in the conventional Sm A phase.[62] On the other hand, the absence of a pyroelectric effect and spontaneous polarization in the chiral polymer excludes completely any tilted smectic structure.

At the same time, to our surprise, P8*M appears visually transparent and nonbirefringent, both in bulk samples and in thin films. This is illustrated by Figure 5.3, where the spot of chiral polymer can hardly be recognized between two glasses in contrast to its racemic isomer, P8$^{\pm}$M. We should stress here that it is impossible to induce any birefringence in P8*M using shear flow, electric field up to 15 V/μm, or magnetic field up to 2.5 T.

P8*M is not the only polymer forming the isotropic smectic phase. To date, we have observed formation of that phase for a half-dozen chiral polymethacrylates and polysiloxanes. Table 5.1 summarizes the chemical structure and phase behavior of synthesized side-chain homopolymers, which carry chirally substituted side chains derived from asymmetric esters of terephthalic acid and hydroquinone. Such a structure with alternating orientation of carboxylic link groups seems to favour the formation of the IsoSm* phase, whereas isomeric derivatives of *p*-hydroxybenzoic acid, where all carboxylic links have the same orientation, form only conventional Sm A and Sm C* phases.[65] Molar mass of all the synthesized homo- and copoly(meth)acrylates is within the range of 1 to $2 \cdot 10^5$ g·mol^{-1}; the polysiloxanes have the average degree of polymerization, $p \sim 35$.

It is worth noticing that the combination of properties of the IsoSm* phase can hardly be explained in terms of known LC phases. The ultrashort pitch TGB-like structure suggested in reference 64 still remains the only structural model that can explain the observed lack of birefringence in the IsoSm* phase.

The twist grain boundary (TGB) phases predicted by Renn and Lubensky[66,67] have been intensively studied in the few last years.[68–71] The general structure of the TGB phase is shown schematically in Figure 5.4. Because the elasticity of the Sm A phase does not allow continuous helical twisting, the chiral superstructure is realized in a stepwise manner: Small smectic grains rotate around a helical axis, while screw dislocations build the

TABLE 5.1 Chiral Homopolymers with Side Chains Based on Asymmetric Esters of Terephthalic Acid and Hydroquinone

Polymer[#]	Main chain	Side-chain structure	n	Phase transitions[†]
P5*A	Acrylate	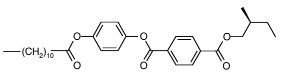		Sm F* 77 Sm C* 97 Iso
P5*M	Methacrylate			gl 40 Sm C* 74 Sm A 85 Iso
P4*A	Acrylate	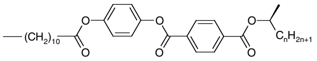	2	Sm B 50 Sm C* 88 Iso
P4*M	Methacrylate		2	gl 40 Sm C* 78 Iso
P6*M	Methacrylate		4	gl 30 **IsoSm*** 53 Iso
P6*ST	Siloxane		4	Sm B 33 Sm C* 51 Iso[‡]
P7*M	Methacrylate		5	gl 30 **IsoSm*** 57 Iso
P7*ST	Siloxane		5	gl 18 **IsoSm*** 54 Iso
P8*A	Acrylate		6	Sm B 55 Sm A 61 Iso
P8*M	Methacrylate		6	gl 30 **IsoSm*** 64 Iso
P8*ST	Siloxane		6	gl 25 **IsoSm*** 61 Iso
P**S	Siloxane	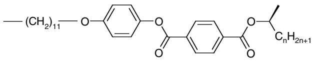	6	gl 24 **IsoSm*** 47 Iso (metastable) or gl 24 Sm C* 43 Sm A 47 Iso (equilibrium)
PL4*A	Acrylate	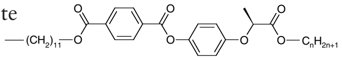	4	gl 10 Iso
PL4*M	Methacrylate		4	gl 15 Iso
PL4*S	Siloxane		4	gl 10 Iso
PL6*S	Siloxane		6	gl 15 Iso

[#] The number in the polymer abbreviations corresponds to the total number of carbon atoms in the chiral terminal group, P stands for polymer, and the last letter relates to the type of polymer main chain. [†] In heating, [‡] For the sample annealed 24 h at 20°C.

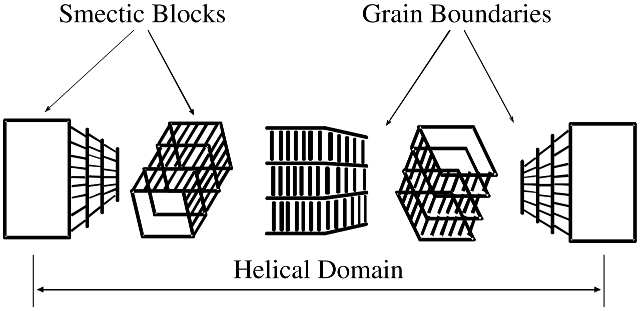

FIG. 5.4 Sketch of the TGB A* structure.

grain boundaries. Within the model, which we suggest for the particular case of the isotropic smectic phase, the small Sm A grains are ~10 nm in diameter, and the helical domains are about 250 to 300 nm long.[64] Thus, all the structural elements are smaller in dimension than the visible light wavelength, and the mesophase appears visually as optically isotropic, in contrast to known TGB A* phases.[72] In the near-UV range, the selective reflection from the TGB lattice cannot be observed, because of the strong absorption of phenyl benzoate groups. The phase still keeps the smectic ordering at the molecular dimensions.

We should state that our suggested model is not completely justified yet, but it remains the only one that can explain the whole ensemble of properties observed for the isotropic smectic phase of P8*M and related polymers. Keeping that in mind, we will refer hereafter to the mesophase as the IsoSm* phase, which most probably has the ultrashort pitch TGB A* structure.

5.3 PHOTOINDUCED BIREFRINGENCE IN PHOTOCHROMIC ISOSM* COPOLYMERS

Because of the combination of short-scale smectic ordering, transparency, and optical isotropy, the IsoSm* phase is promising for numerous optical and photo-optical applications. We therefore prepared three series of copolymethacrylates combining the monomer matrix of P8*M with dichroic comonomers based on different azobenzene dyes, namely *p*-cyanoazobenzene (SK series), *p*-mehoxyazobenzene (KW series), and *p*-trifluoromethoxyazobenzene (KM series).[73,74] Figure 5.5 presents the chemical stuctures of the comonomer units and the corresponding range of compositions, where the formation of the IsoSm* phase is observed. The copolymers are referred to as SK*n*, KW*n*, and KM*n*, respectively, where *n* is the concentration of azo dye comonomer, mol. %. For all three copolymer series, the corresponding phase diagram can be divided in three sections. At lower *n* values, the copolymers form an equilibrium IsoSm* phase, whereas at higher dye concentration they form a conventional Sm A phase. The intermediate range of concentrations corresponds to the metastable formation of the IsoSm* phase, which is formed at fast cooling (≥ 15 K/min), whereas slow cooling results in formation of an Sm A phase. Thus, a copolymer can appear at ambient temperature

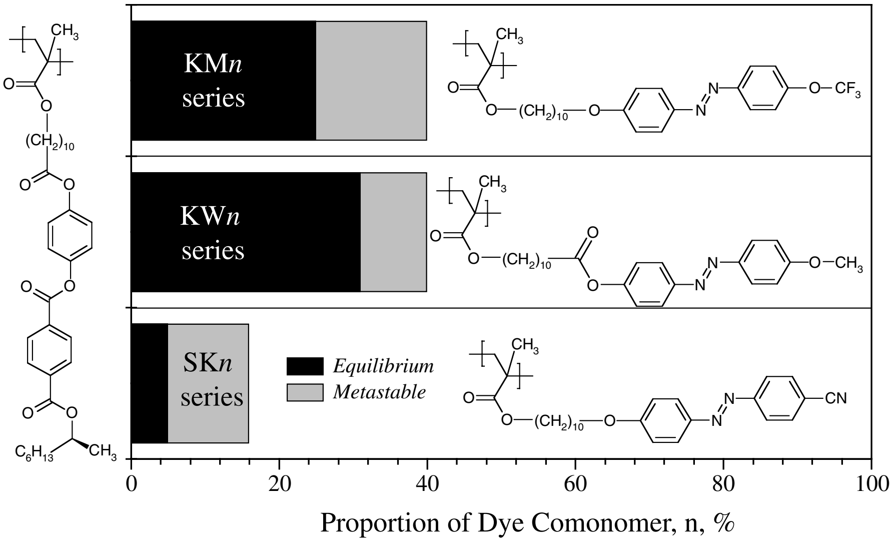

FIG. 5.5 Range of compositions favoring the formation of the IsoSm* phase for chiral azo dye side-chain copolymers.

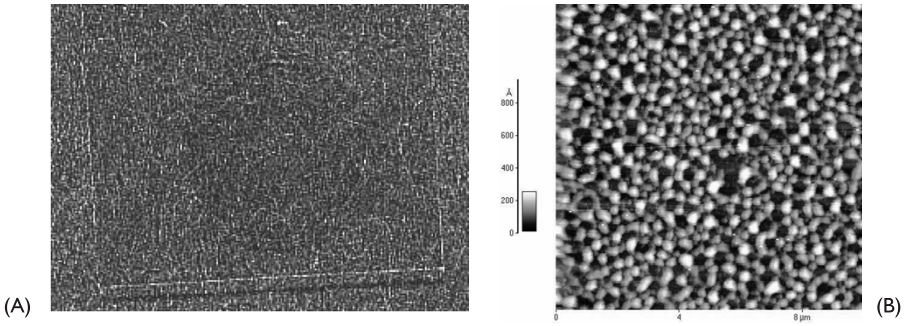

FIG. 5.6 (A) Optical appearance of an azo dye IsoSm* film (KW11); (B) surface relief of an azo dye IsoSm* copolymer (KW40, cast film).

either as high-transparent, optically isotropic IsoSm* glass, or as turbid, scattering, and birefringent Sm A glass, depending on sample prehistory. We should underline here that particularly in that intermediate range of copolymer proportions, the phase transformations can be controlled by light illumination during cooling, thus allowing the LCPT recording (see Section 5.6).

As seen from Figure 5.5, the chiral dye copolymers form the IsoSm* phase in a broad range of compositions. The phase appears orange in colour but transparent, amorphous, and elastic (Figure 5.6A), in contrast to the turbid, birefringent, and fragile polydomain texture of Sm A copolymers with a higher proportion of dye moieties. At the same time, the AFM profile of a free surface of a photochromic IsoSm* copolymer[75] shows a grain texture with the periodicity of 250 nm (Figure 5.6B), thus giving more evidence for the suggested short-pitch TGB structure of the mesophase.

It should be noted that the Iso → IsoSm* phase transition on cooling is thermodynamically controlled for the former two series but kinetically controlled for the KM series.[74] As an example, Figure 5.7A presents DSC data from KM11. As seen from the figure, the second DSC scan from the polymer sample shows no transition peaks, but glass transition inflexion only; the

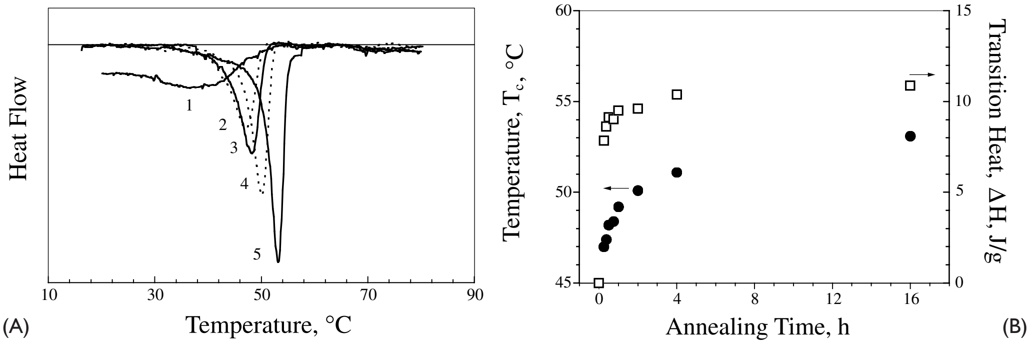

FIG. 5.7 (A) DSC curves from KM11: (*1*) second scan (no annealing), (*2–5*) sample annealed at 32°C for 0.25 h, 0.5 h, 2 h, and 16 h, respectively; (B) corresponding growth of the transition temperatures (●) and enthalpies (□) with the annealing time.

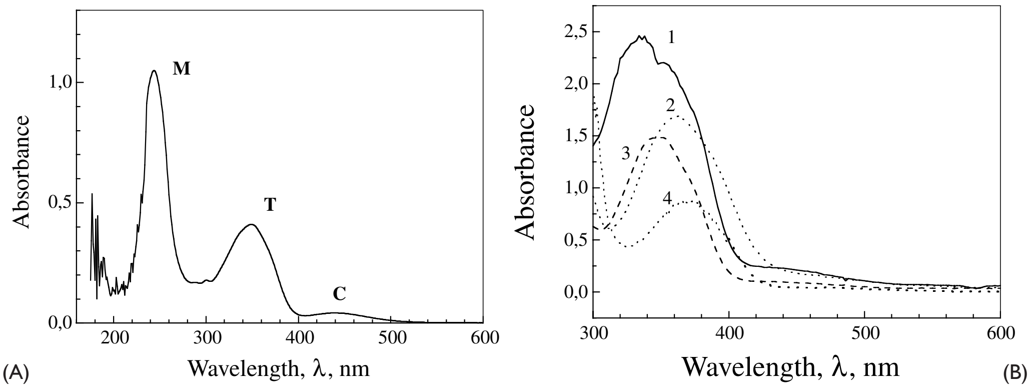

FIG. 5.8 Absorption spectra of the photochromic IsoSm* copolymers: (A) KW40 (chloroform solution, 12 mg/l); (B) spin-coated films of (*1*) KM55, (*2*) SK28, (*3*) KW40, and (*4*) SK5.

transition peak can, however, be recovered with sample annealing. The corresponding growth in the transition temperatures and enthalpies with annealing time is shown in Figure 5.7B. It is clearly seen that the transition is completed within about one day.

The copolymers manifest three characteristic spectral bands in UV-vis absorption spectra (see Figure 5.8A): Band **M** at about 240 nm corresponds to the absorption of mesogenic phenyl benzoate groups; band **T** at about 330 to 370 nm (for different copolymer series, see Figure 5.8B) relates to the π-π* transition in the *trans*-isomer of the azo chromophore; and less developed band **C** at 440 to 460 nm to the n-π* transition.[76–78] We should comment here that for individual molecules, band C is allowed only for the bent *cis*-isomers, the number of which is very small under ambient conditions. On the other hand, the selection rule might be cancelled by the interaction of the chromophores with the surrounding medium, and the elongated *trans*-isomers might be allowed to participate in the band C absorption. Our study shows, for instance, that for SK8, the n-π*oscillator strength of a *cis*-isomer (allowed by symmetry) in a thin film is only two times higher than that of the *trans*-isomer (forbidden in the simplest model).[77]

Furthermore, the copolymers show pronounced photochromism, similar to other azobenzene derivatives: UV irradiation transforms most of the azobenzene units from the *trans*-isomer to the *cis*-isomer, so that the band **T** disappears but the band **C** increases considerably (see Figure 5.9A), wheres the backward isomerization occurs thermally in darkness but can be accelerated by yellow light irradiation (see Figure 5.9B). Once again, we should note that a strong illumination by green light (within the band C) can result in the *trans-cis* transformation because of the n-π* transition, as considered in the previous paragraph. The process is not as efficient as the π-π* transition under UV irradiation but, nevertheless, it shifts slightly the equilibrium ratio between the isomers in favour of *cis*-isomers.

We should underline here one peculiarity of the chiral photochromic copolymers under discussion: The *cis*-isomers have an extremely long lifetime

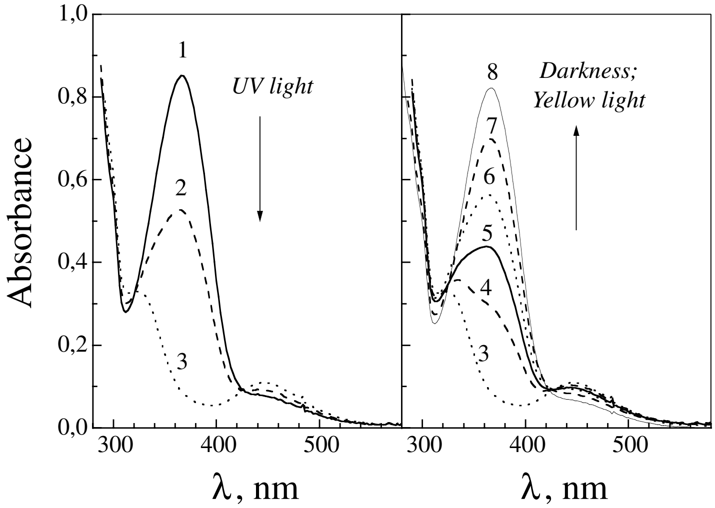

FIG. 5.9 (A) Changes in the UV absorption spectra of copolymer films under UV irradiation. (B) Dark relaxation and yellow light illumination afterwards (1) virgin film; (2) UV illumination for 5 s; (3) the same for 30 and 60 s; (4–7) dark relaxation for 3 min, 6 min, 9 min, and 24 h, respectively; (8) illumination with yellow light, 30 s.

as compared with other photochromic materials based on azobenzene derivatives, including low molar mass chiral dyes and achiral LC polymers (see Table 5.2). This opens up the possibility of preparing thin polymer films (both cast and spin-coated) in their *cis*-form, from UV-irradiated solutions. After evaporation of the solvent, the films keep the acquired *cis*-form for hours and can be further used for photorecording purposes.[77]

As mentioned in Section 5.1, the reorientation of azobenzene photochromic moieties under illumination with polarized light and the birefringence that is induced from it are well known and covered in many publications.

TABLE 5.2 Lifetime of cis-Forms for Various Azobenzene Derivatives

Azo-dye compound	**Temperature, °C**	**Relaxation time, τ**	**Reference**
Chiral low molar mass dye			
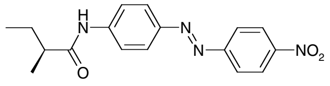	25	~ 3 min	79
Achiral LC polymer			
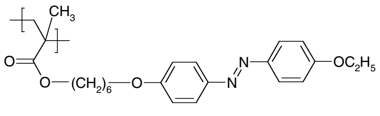	50	~ 2. 5 min	52
Chiral LC copolymer			
SK8	20	2.5 h	76, 77
KW40	20	10 h	76, 78, 80

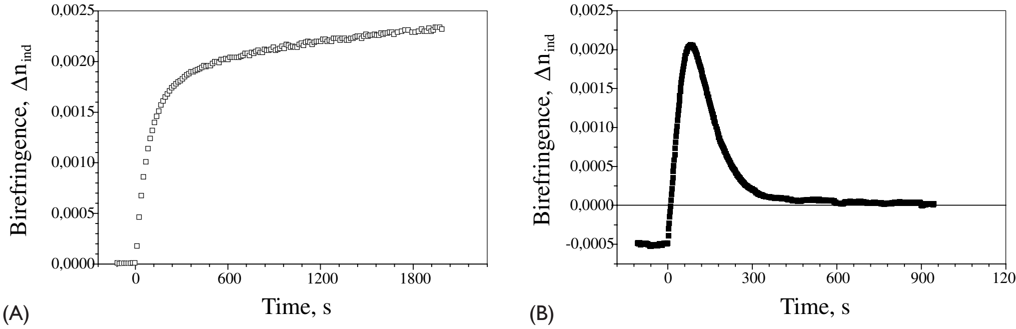

FIG. 5.10 (A) Evolution of the birefringence, Δn_{ind}, induced by polarized blue-green light ($400 < \lambda < 500$ nm) in a 19- μm-thick KW40 film; (B) the same, in a 3-μm-thick film, induced by UV light (initial birefringence of the film induced by preliminary illumination with polarized blue-green light).

The value of the photoinduced birefringence, Δn_{ind}, the kinetics of its growth under illumination, and its stability thereafter depend on many factors, including the chemical structure of the azobenzene dye and of the polymer matrix, light intensity, wavelength, temperature, film thickness, etc. As an example, Figure 5.10A presents the growth of the Δn_{ind} values with illumination time in a 19 μm thick pressed film of KW40.[81]

The plot presented in Figure 5.10B gives evidence that polarized UV light, in contrast to visible light, induces birefringence in azo dye copolymer films only at the initial step of the irradiation, whereas further illumination results in disappearance of the phase retardation. This effect can be explained by the complete and reversible reorientation of both chromophores and mesogenic units along the light wave vector, as discussed by Han *et al*.[78,82]

The effect of illumination wavelength (within the visible range) on the photoinduced birefringence is shown in more detail in Figure 5.11. As seen in the figure, when cutting off the wavelength range below $\lambda \sim 500$ nm, one cannot induce any further birefringence. On the other hand, the blue-violet light ($\lambda < 420$ nm) seems to have a negligible effect on the Δn value (see Figure 5.11B). We can conclude, therefore, that the irradiation within absorption band **C** (Figure 5.8) is responsible for the long-term photoinduced birefringence, as shown in Figure 5.10A.

The dependence of photoinduced birefringence on light intensity, as presented in Figure 5.12, shows saturation at 150 to 200 mW/cm^2. It should be noted, however, that the Δn_{ind} values saturate versus the irradiation power but not versus the illumination time (Figure 5.10A).

Of considerable importance is also the fact that nonpolarized UV irradiation can erase completely the previously induced birefringence, newly writing another pattern. As seen in Figure 5.13, irradiation of a UV-treated copolymer film by *p*-polarized visible light results in a negative phase delay, a subsequent irradiation with nonpolarized UV light eliminates birefringence, and subsequent irradiation by *s*-polarized visible light induces positive birefringence.

When comparing the data of Figure 5.13 with those from Figure 5.10A for the same film thickness (curve 2), it is clearly seen that the preliminary

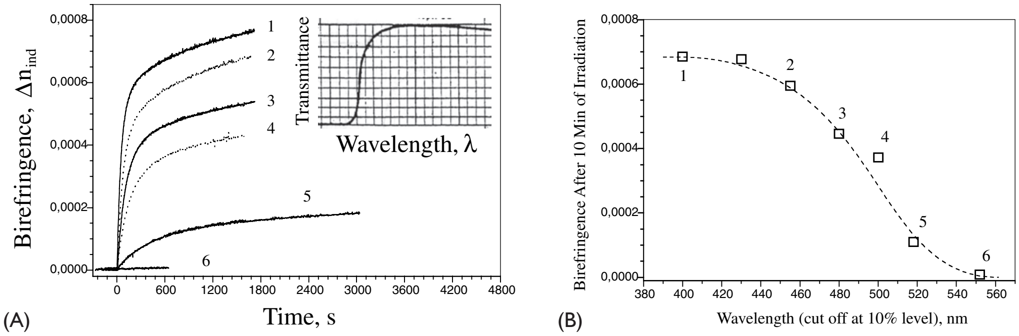

FIG. 5.11 (A) Evolution of the birefringence, Δn_{ind}, induced by polarized light in a copolymer film (KW07, 23 μm) through color filters with different transmission ranges. Typical transmission curve of a filter shown as insert; (B) The Δn value induced for 10 min, versus the wavelength corresponding to the filter transmission 10%. Point numbers correspond to the curves in Figure 5.11A.

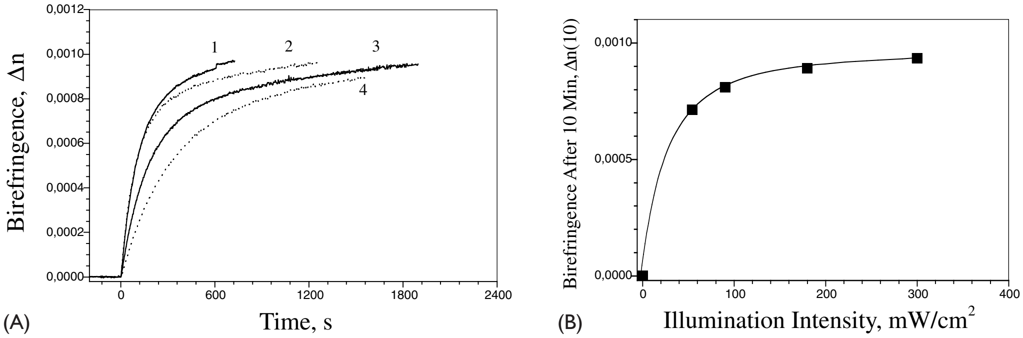

FIG. 5.12 (A) Evolution of the birefringence, Δn_{ind}, induced by polarized white light in a copolymer film (KW19, 22 μm) without filters (*1*) or through grey filters of different optical density (*2–4*); (B) the Δn value induced for 10 min, versus the light intensity.

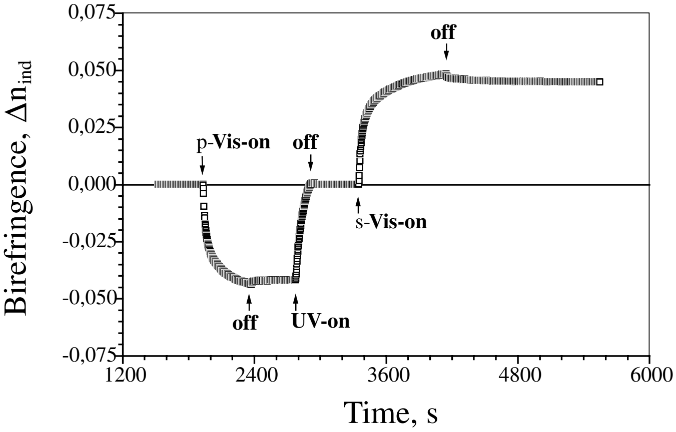

FIG. 5.13 Evolution of the induced birefringence in a dye copolymer film (KW40, 3 μm) under consequent irradiation with *s*-polarized blue-green light, UV non-polarized light, and *p*-polarized blue-green light.

irradiation with nonpolarized UV light increases drastically the birefringence induced by polarized visible light: $\Delta n_{ind} \approx \pm 0.045$ for the illuminated film versus $\Delta n_{ind} \approx \pm 0.001$ for that reached without UV treatment. This gives rise to the possibility of amplifying the sensitivity of the material to visible light by previous exposure to UV light. To some extent, the phenomenon is similar to the "nonvolatile holographic storage effect" observed recently in a doubly doped inorganic ferroelectric.[83] Our data show, however, that the UV sensibilization is much more pronounced for the copolymers of the KW series[78–80,84] than for the SK and KM series.[77,81] That can be explained by the stronger electron-accepting substituents at the tail of the azobenzene chromophores for the latter two series, –CN for SK copolymers and $-OCF_3$ for KM copolymers as compared with $-OCH_3$ for KW copolymers, which lead to reduced stability and shorter lifetimes for the *cis*-isomers, as reported by Ikeda *et al.*[50–52]

There is one more possibility for substantially increasing the stability of photoinduced birefringence in chiral LC copolymers. If the light-induced reorientation of photochromic azo groups occurs not in a well-formed (mature) mesophase, but during phase formation, it is less restricted by main-chain conformation, so that higher Δn values can be achieved. Moreover, corresponding structural reorganization should involve the polymer main chain itself. As a result, its conformation "memorizes" the preferred orientation of chromophores and the thereby-induced cooperative reorientation of colorless mesogenic moieties in glass, and the copolymer film keeps the macroscopic orientation for much longer times.[85]

Table 5.3 compares Δn values recorded in a 22-μm film of KW19 after 20 min of irradiation with polarized white light from a polarizing microscope for isothermal recording at 26°C and recording during sample cooling from 66 to 26°C. It is clearly seen that the thermally assisted recording is twice as efficient and much more stable. To illustrate the stability of such an "imprinted" birefringence (i.e., photoinduced during film cooling), Figure 5.14 presents a 2.5-year-old birefringent spot, induced in the copolymer film during microscopic observations.

The kinetically determined Iso–TGB A* phase transition in copolymers of the KM series (shown in Figure 5.7) allows also for isothermal nonequilibrium photorecording in the copolymers. Figure 5.15 shows the evolution of photoinduced birefringence in a film just cooled from 100°C, where the

TABLE 5.3 Comparison of the Isothermally Recorded and "Imprinted" Birefringence in Dye Copolymer Film (KW19, 22-μm Film)

Birefringence, Δn	Isothermal recording (20 min at 26°C)	Thermally assisted recording (20 min as cooledfrom 66°C to 26°C)
Immediately after the recording	0.0008	0.0020
18 h later	0.0003	0.0019

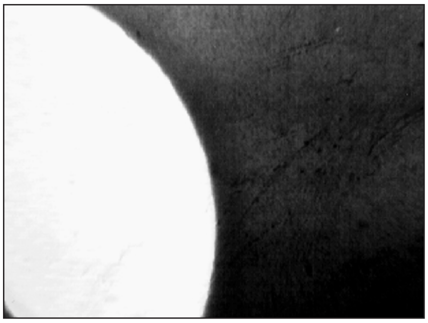

FIG. 5.14 Microphotograph of a 2.5-year-old photorecorded birefringent spot (left) in ~20-µm-thick film of SK8.

mesophase is still being formed with time, as compared with the birefringence induced under the same conditions in a film kept for 24 h at ambient temperature, where the short-pitch TGB A* phase is already organized completely. As seen from the figure, the illumination during the mesophase formation results in Δn_{ind} values that are three times higher.

We should emphasize that by using thick but still transparent IsoSm* films, we can obtain huge phase delay even for moderate Δn_{ind} values. For instance, the maximum value of the photoinduced birefringence shown in Figure 5.15 (curve 1) was measured for a 24-µm-thick film and corresponds to the phase delay value $\Delta\Phi = -245°$, i.e., close to the three-quarter-wave plate.

To summarize, photochromic chiral IsoSm* copolymers are capable of photoreorientation under illumination with polarized light. If irradiated within the UV wavelength range (band T), the Δn_{ind} value achieves maximum

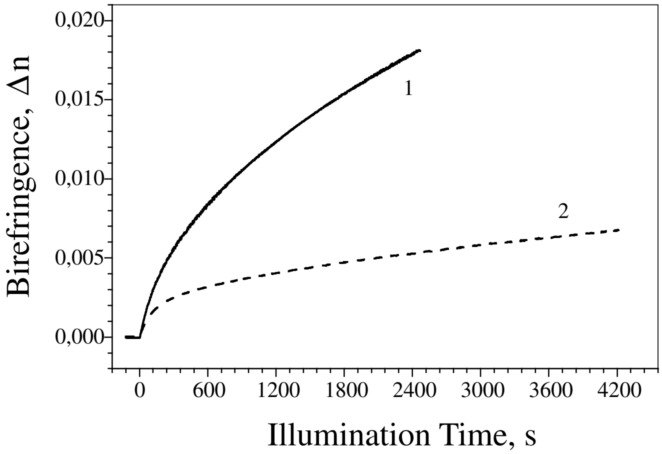

FIG. 5.15 Growth of the photoinduced birefringence in (*1*) just-cooled and (2) 1-day-old copolymer films (KM25, 23 µm) under light illumination (nonfiltered white light, 0.3 W/cm^2).

within 1 to 2 minutes but disappears if the irradiation is continued further. On the other hand, the birefringence induced by blue-green light (band C) shows no saturation, due to repeated *cis-trans-cis* transformations. The sensitivity of films to visible light can be substantially increased by preillumination with nonpolarized UV light. Photorecording during the phase formation (on cooling, or also during the kinetically determined isothermal mesophase formation for copolymers of the KM series) results in much higher Dn_{ind} values as compared with photorecording in a completely organized mesophase.

The combination of these features presents photochromic IsoSm* films as interesting and diverse media for optical data storage. In Section 5.4, we consider holographic grating recording in copolymer films and related (combined) photorecording techniques.

5.4 HOLOGRAPHIC GRATING RECORDING

Optical holography provides unique opportunities for information storage and visualization. To date, most investigations have focused on doped inorganic crystals,[86] the polymer organic materials attract more and more attention as holographic media, however, because of easy processing and "custom-tailored" adjustment of properties with well-developed polymer technology techniques. Among those, amorphous and liquid crystalline azobenzene side-chain polymers[9–42] are distinguished for high diffraction efficiency, easy erasing/rewriting of recorded data, and reasonably short response time.

Generally, there are three mechanisms for writing holograms in azo-dye polymers: (1) (rotational) molecular reorientation; (2) redistribution of *cis*- and *trans*-isomer population; and (3) formation of surface relief grating.[56,87] The first two mechanisms represent bulk effects, and the latter is related to the surface. The contribution of these mechanisms into the total diffraction efficiency depends on many parameters, including the extinction coefficient at a particular wavelength of a laser beam, the quantum yield of the photochemical isomerization, the temperature-dependent relaxation time of the *cis*-isomers, the angular diffusion, or even the film confinement conditions. To elucidate the mechanism of photorecording, and to optimize the conditions for readout of recorded data, different polarization geometries of the interfering pump beams can be chosen.[84,87]

Holographic grating recording in the chiral photochromic copolymers of the SK-, KW-, and KM-series has been studied for several polarization configurations. Figure 5.16A shows the experimental setup for the grating recording, and the light-field interference patterns for *s,s*-, *p,p*-, *s,p*-, and *R,L*-configurations of laser beams are presented in Figure 5.16B. Here, *s*- and *p*-polarizations correspond to linear polarization with the electric vector of the incident beam perpendicular and parallel to the plane of light incidence, whereas the *R*- and *L*-polarizations correspond to right- and left-handed circularly polarized light. The experimental scheme of Figure 5.16A allows for all four types of recording with the proper choice of waveplates, WP. Some examples of holographic gratings recorded in an IsoSm* copolymer film are shown in Figure 5.17.

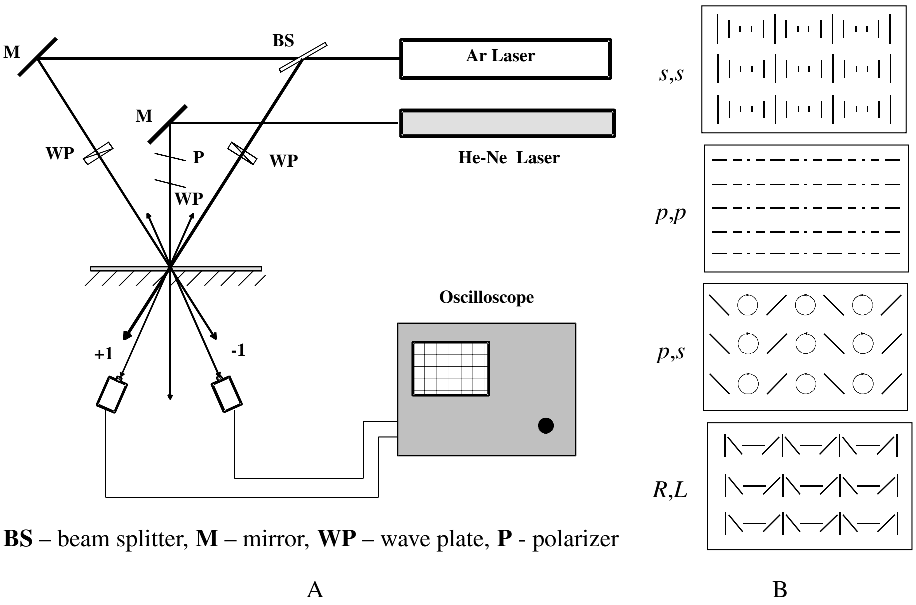

FIG. 5.16 (A) Experimental setup for holographic grating recording; (B) schematic representation of electric field patterns on a vertically installed sample.

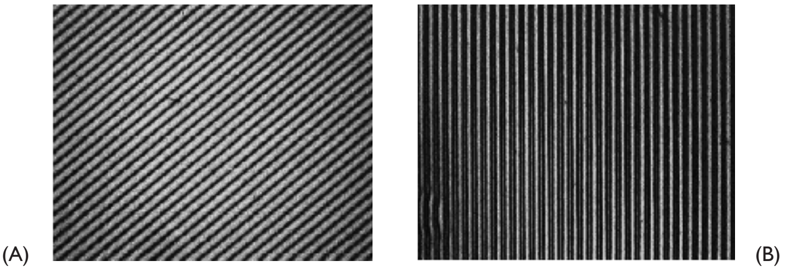

FIG. 5.17 Microphotographs of an (A) *s,s*-grating and a (B) *s,p*-grating from SK8 (22-µm pressed film) in crossed polarizers.

The quality of holographic grating is estimated by the efficiency of the probe beam scattering from the grating, calculated as the ratio of light intensities for the first diffraction order and for the incident beam, $\eta = I_1/I_0$. The He-Ne laser source is usually selected for the probe beam, because it is inactive in the photochemical processes involved. The η value depends substantially on the wavelength and intensity of the recording beam, the recording time, and the prehistory of the sample.

It has been shown that the scattering efficiency of the grating recorded in a 23 µm thick virgin film of SK8 grows linearly with the exposure time at constant beam power but falls drastically with the wavelength of the recording beam.[77] In contrast, the η value shows a superlinear growth upon

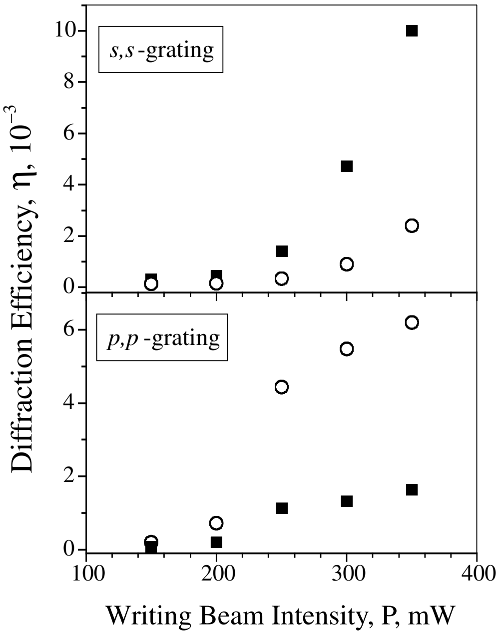

FIG. 5.18 First-order *s*- and *p*-diffraction efficiencies (■ and ○, correspondingly) of *s,s*- and *p,p*-gratings recorded with a fixed exposure time, t_w = 15 s, as a function of the power of the initial *s*-polarized (top) and *p*-polarized (bottom) Ar laser beam (for the ∅ 1.6-mm spot).

increase in the beam intensity, for a fixed exposure time, as shown in Figure 5.18. The superlinearity is especially pronounced at higher writing powers. The data presented in the figure show unambiguously that in the cases of both *s*,*s*- and *p,p*-gratings, the diffraction efficiency of the probe beam is higher for polarization coinciding with that of the writing beams. On first sight this looks strange because, in uniaxially symmetric materials, the difference $n_\parallel - n_{\mathrm{iso}}$ is always larger than $n_\perp - n_{\mathrm{iso}}$ (n_{iso}, $n_\parallel$, and $n_\perp$ are refraction indices for the nonoriented phase, and parallel and perpendicular to the director, respectively), and if the chromophores are deviated outwards of the light electric vector into the perpendicular position, the difference δn between illuminated and dark parts would be greater for the perpendicular polarization. However, a more precise analysis of a simple three-dimensional model[88] shows that what we observe here is a typical situation when the angular distribution of chromophores in darkness is close to isotropic (the case of the chiral optically isotropic TGB A* phase, IsoSm*).

At the same time, only low-contrast *s*,*s*- and *p*,*p*-gratings could be written at $\lambda = 514$ nm in a virgin 3-μm-thick film of another copolymer, KW40, using a power of the output Ar laser beam as high as 25 W/cm^2 (writing time t_w=2s).[78] However, as was mentioned in Section 5.3, pretreatment with unpolarized UV light increases the proportion of long-living *cis*-isomers and amplifies therewith the photo-optical response, the effect being especially pronounced for the copolymers of KW series with lower longitudinal dipole moment of the photochromic groups. Thus, film sensibilization with UV pre-

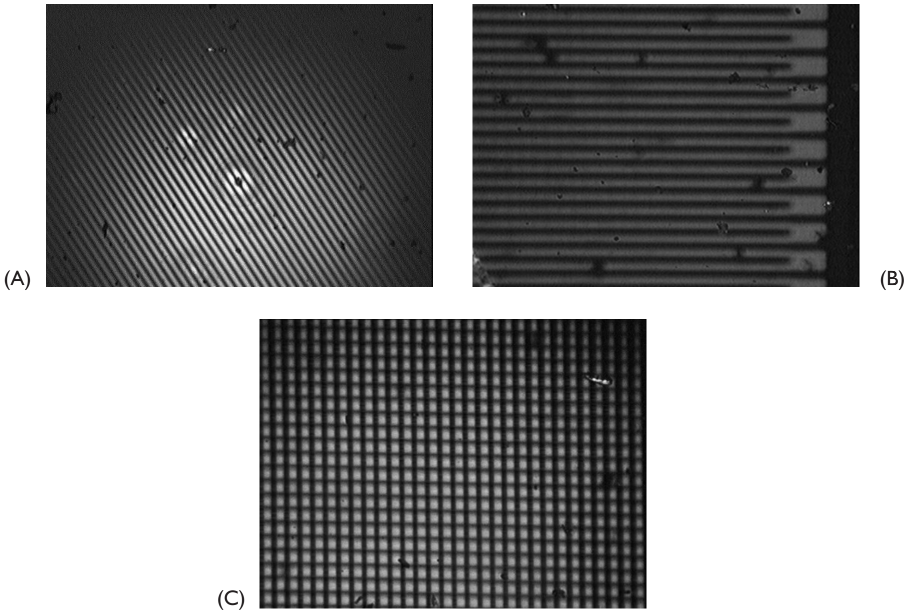

FIG. 5.19 (A) Image of a holographic grating recorded on a UV-sensibilized KW40 film (grating period is 38 μm). (B) Image of a mask recorded by unpolarized UV light and developed by polarized visible light (grating period is 40 μm). (C) Holographic development (grating period is 38 μm) of an image of mask with grating period 40 μm.

treatment (2 mW/cm^2 at $300 < \lambda < 400$ nm) gives a 100-fold gain in the exposure for holographic gratings, which can easily be recorded with a power density of less than 0.5 W/cm^2 and t_w=1s. An image of such a grating is shown in Figure 5.19, and Figure 5.20 (left) shows the diffraction efficiency, η, from the *s,s-* gratings versus writing time. The maximum diffraction efficiency is reached within 3s, η_{max} = 0.27%. In contrast to the efficiency reported previously for SK8 films, the diffraction efficiency is higher for the orthogonal polarization of the recording and probe beams. This might be explained by a different mechanism responsible for the modulation of the birefringence index in the gratings for the two copolymers—namely, enrichment and depletion of the material with *cis*-isomers should play the key role for KW40, but the photoinduced reorientation of chromophores, similar to the mechanism reported for Langmuir-Blodgett films of low molar mass azo dyes, plays the Key role for SK8.[88]

As the proportion of *cis*-isomers relaxes thermally to the equilibrium state, the enhanced sensitivity of the film to the writing beam degrades completely, for about 10 hours at ambient temperature (the lifetime of *cis*-isomers). The desensibilization process may be accelerated by additional exposure of the film to the white light of an incandescent lamp, as shown in Figure 5.20, right (power density 2 mW/cm^2 in the range 450 to 650nm): A 30 min irradiation is sufficient to suppress the sensitivity by converting all *cis*-isomers into their *trans*-counterparts. It is of great importance, nevertheless,

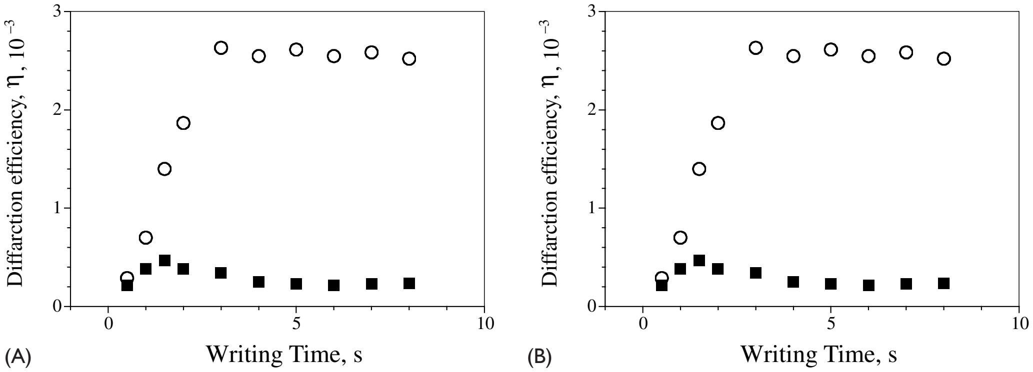

FIG. 5.20 (A) Diffraction efficiencies, η, of *s,s*-gratings in the 10 μm thick KW40 film, as read out by an *s*- (■) or *p*- (○) polarized probe beam, versus writing time. (B) Grating diffraction efficiencies, η_p, for the *p*-polarized reading beam, as functions of the writing time. After UV irradiation (t_{exp} =0), the film was exposed additionally to the light of an incandescent lamp, and gratings were recorded at different exposition times, t_{exp}, shown at the curves.

that a grating, once recorded, remain stable for a much longer time (several weeks under ambient conditions) even when all the *cis*-isomers have already converted into the *trans*-form. And moreover, under the strong additional illumination by visible light that eliminates *cis*-isomers, the grating remains stable.

The UV-sensibilization of copolymer films also allows the possibility of writing hidden images as sensibilized patterns in an "inert" (much less sensitive) area by UV illumination through a mask. The film remains visually isotropic and uniform, but the image can be developed later by illumination with polarized visible light. As an example, Figure 5.19B presents the pattern recorded with unpolarized UV light ($300 < \lambda < 400$ nm, exposition 10 min, power density 3.3 mW/cm^2) and developed with polarized blue-green light ($400 < \lambda < 500$ nm, power density 5 mW/cm^2). Moreover, if the developing illumination with visible light is not uniform, the resulting image represents the overlap of recording and developing patterns, as shown in Figure 5.19C.

We should point out that photochromic IsoSm* films are even more sensitive to holographic grating recording with circularly polarized light (*R,L*-gratings), as compared with *s,s*-, *p,p*-, or *s,p*-gratings recorded with linearly polarized light (see Figure 5.16B for the corresponding interference patterns). The interference of two coherent beams having opposite circular polarizations creates no intensity modulation, but only a rotation of the linear polarization in the interference plane;[87] a comprehensive theoretical consideration is given by Cipparone *et al.*[84] Thus, virgin spin-coated ~0.25-μm-thick films of KW40 allow for recording a phase grating at a beam power density as low as 0.5 W/cm^2, as compared with the 25 W/cm^2 required for a *p,p*-grating in the same polymer (without the sensibilization). The gratings are unstable, however, and degrade within several minutes when recorded under low beam intensity. As an example, Figure 5.21 illustrates the decay of diffraction intensity from an *R,L*-grating recorded in a spin-coated film of

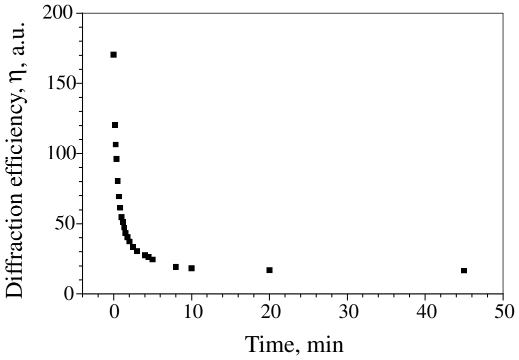

FIG. 5.21 Relaxation of the phase grating (SK8; ~ 0.25-μm spin-coated virgin film; writing beam 0.5 W/cm^2 at λ = 514 nm for 5 min) after switching off the pump beam.

SK5. Two relaxation domains, the fast one with $\tau_1 \sim 10^1$ min and the slow one with $\tau_2 \sim 10^3$ min, can be recognized in the figure.

On the other hand, images recorded with higher power density or in UV-sensibilized IsoSm* films (see Figure 5.17 and 5.19) are stable under ambient conditions for at least months. It is possible to erase them, however. Heating the polymer to above the phase transition point (~60 to 65°C) and illumination with unpolarized UV light both erase any recording and make the same spot ready for new recording (as shown in Figure 5.10B). We made several such cycles on the same spot without any trace of material degradation. This is consistent with observations that polymer films with azo compounds can survive thousands of *trans-cis-trans* photoisomerisation cycles.[89] On the other hand, a grating may be erased using a single Ar laser beam providing a spatially uniform illumination. An example is shown in Figure 5.22. The grating in SK8 film was recorded with two beams of initial nonsplit beam power at 15.4 W/cm^2 and for t_w = 15 s and erased with a single beam of 6.2 W/cm^2. Almost complete erasure was achieved at ~ 50 s.

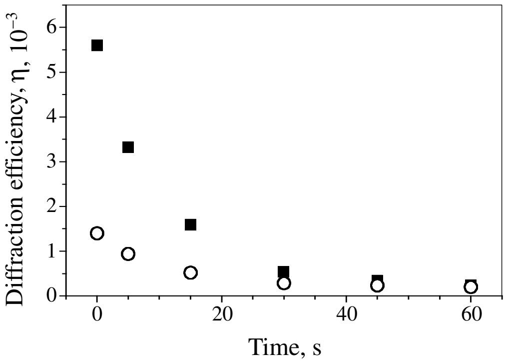

FIG. 5.22 First-order *s*- and *p*-diffraction efficiencies (□ and ○, correspondingly) of the s,s- grating written in SK8 (23-μm film), as functions of the "erasing time".

We conclude this section with the remark that high-transparent, optically isotropic, chiral and photosensitive IsoSm* copolymers represent novel and versatile media for holographic grating recording, allowing UV sensibilization, recording of both intensity and phase gratings, and holographic development of hidden sensibilization patterns.

5.5 PHOTOINDUCED ALIGNMENT OF LOW MOLAR MASS LIQUID CRYSTALS

In recent years, many studies have been devoted to the photoinduced alignment of nematic liquid crystals by photosensitive polymers. Advantages of this technique for optoelectronic technology are quite evident in comparison with such traditional methods as mechanical buffing of an orienting polymer layer: It is a “clean” technique that may be applied not only to flat substrates, but also to curved ones or even those not accessible to mechanical contact at all. In addition, buffing is irreversible, but photoinduced liquid crystal alignment may be changed optically. It may also be combined with buffing.

The most popular photoalignment technique is based on photo-crosslinking various poly(vinylcinnamates), PVC.[90,91] The initially optically isotropic PVC layer, which provides a degenerate planar alignment of a nematic liquid crystal (NLC), becomes optically anisotropic due to a lack of chromophores in a direction selected by polarized UV light and orients the NLC *perpendicular to the light electric vector*. The same alignment occurs when rod-like azo dyes are reoriented by light action.[92] On the other hand, NLC alignment *parallel to the light electric vector* may be achieved using coumarin dye layers.[93,94] This case is more interesting because, for reasons of symmetry, it is possible to produce an orientation of nematics with an arbitrary tilt angle using an oblique incidence of the exciting light. In both cases mentioned in this paragraph, only two different orientations of a liquid crystal are possible: degenerate planar (initial), and uniaxial either along or perpendicular to the light vector.

We tested the azo dye IsoSm* copolymer, KW40, as a photo-orienting layer for low molar mass nematic liquid crystals MBBA, 5CB, and E7. The studies were done using hybrid liquid crystal cells made of 1 mm thick ITO covered glass plates transparent in the range of $\lambda > 350$nm. Hybrid cells are the most convenient cells for anchoring energy determination because, in the high field limit, the field-induced distortion is easily modelled by the semi-infinite medium.[95] The homeotropic orientation was made using a surfactant chromium distearyl chloride (chromolane). On the opposite plates, spin-coated films of KW40 of different thicknesses (100 to 600 nm) were deposited from a 1 to 2% cyclohexanon solution of the copolymer. The films were irradiated by normally incident polarized UV or visible light before filling the cell with a liquid crystal.

The initial texture of a hybrid cell filled with E7 is seen outside the dark spot in Figure 5.23. It is a typical texture of a hybrid cell with *degenerate planar anchoring*. Such texture was also observed for MBBA and 5CB. After strong irradiation with UV light (either polarized or unpolarized; it does not matter) corresponding to the end of the curve shown in Figure 5.10B, a

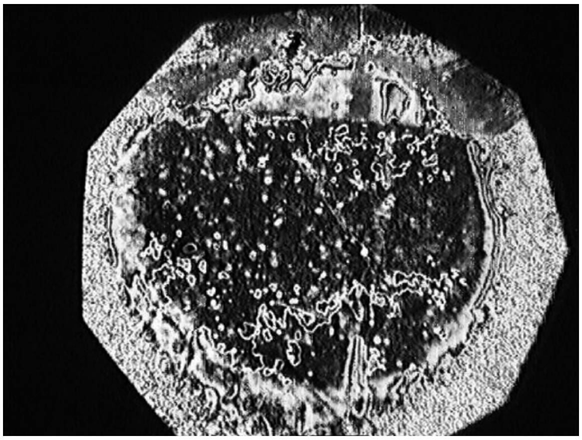

FIG. 5.23 Microphotograph of a 3.3-mm-diameter spot (dark on the bright background) of NLC E7 oriented with the director along the electric vector of exciting UV light. Hybrid cell, 11.5 µm, the KW40 layer was irradiated for 7 s with polarized UV light (160 mW/cm^2, λ = 300-400 nm) before filling the cell.

homeotropic texture is observed. If however, the irradiation of the copolymer film by polarized UV light is stopped in a few seconds (around the maximum shown in Figure 5.10B), after filling the cell a *homogeneous* orientation is observed with the *director oriented parallel to the UV light electric vector*. It is seen between crossed polarizers as a dark spot on the bright background of the degenerate planar texture (see Figure 5.23). There are two types of defects observed for E7, 5CB, and MBBA. One of them is typical of hybrid cells without a pretilt angle at the planar interface: Different domains having opposite splay-bend curvatures are separated by disclination lines. The other type, similar to long brushes, originates from the considerable solubility of our copolymer in liquid crystals: Some material is washed out while is being filled.

Finally, a *homogeneous* orientation is observed with the *director oriented perpendicular to the light electric vector* if the layer was pretreated with strong UV light and additionally irradiated by *s*- or *p*-polarized visible light. This case corresponds to the plateau regions (either positive or negative) visible in Figure 5.13. The textures are similar to those shown in Figure 5.6.

Because the homogeneous orientation with the director oriented parallel to the light electric vector is the more rare and interesting, the anchoring energy measurements were carried out for this latter case. Figure 5.24 shows the experimental optical path difference, $R = <\Delta n>d$, as a function of the following electric coherence length:

$$\xi = \frac{1}{E}\left(\frac{4\pi K}{\varepsilon_a}\right)^{1/2} \tag{5.1}$$

In this equation, ε_a is the dielectric anisotropy, $K = (K_{11}+K_{33})/2$ is an average splay-bend elastic modulus, and E is the applied electric field. In this presentation, the curve must be linear when the Rapini approximation for the

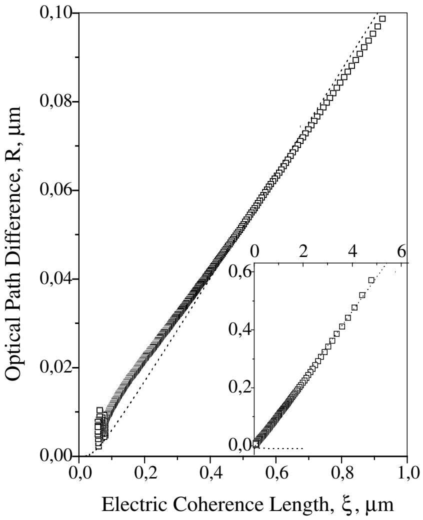

FIG. 5.24 Optical path difference, *R*, versus the coherence length, ξ, for a 23-µm-thick hybrid cell filled with E7 [homeotropic boundary: chromolane; planar boundary: KW40 irradiated for 3 s by polarized UV light of intensity 160 mW/cm^2 ($\lambda = 300 - 400$ nm) before filling cell.] Insert : Large scale for ξ, $\xi = 0 - 6$ µm. Main plot: Strong field region, $\xi = 0 - 1$ µm.

anchoring energy is used and the flexoelectricity is not taken into account.[96] Actually, the curve for a rather large range of ξ seems to be linear (see the insert in Figure 5.24).

The more careful fitting of the $R(\xi)$ curve to the two-dimensional theoretical model[95] is shown by the dotted curve in the insert. All measurements were made at temperature 29 to 30°C and the following parameters of E7 were used for calculations: refraction indices $n_{\parallel} = 1.7238$, $n_{\perp} = 1.5185$; dielectric susceptibilities $\varepsilon_{\parallel} = 18.6$, $\varepsilon_{\perp} = 5.1$; elastic moduli $K_{11} = 1.04 \cdot 10^{-6}$ dyn, $K_{33} = 1.69 \cdot 10^{-6}$ dyn. The curve corresponds to anchoring energy $W \approx 1$ erg/cm^2 and the apparent pretilt angle $\vartheta_{app} = 7°$. For the normal incidence of UV irradiation, the pretilt angle should not appear. In fact, a finite ϑ_{app} reflects the inhomogeneous (domain) structure with out-of-plane (three-dimensional) distortion of the hybrid cell. In the main plot, the experimental and theoretical curves are given in the strong field limit. A remarkable deviation from the simple theory is observed, as was the case with buffed polyimide orienting layers.[95] This is probably related to some flow phenomena induced by a strong electric field.

5.6 PHOTOAFFECTED PHASE BEHAVIOUR AND THE LCPT PHOTORECORDING

As mentioned earlier in this chapter, the elongated *trans*-form and the bent, banana-shaped *cis*-form of the same azobenzene chromophore differ substantially in molecular dimensions and therefore can reveal quite different phase behaviour. We have found that, in the case of chiral photochromic copoly-

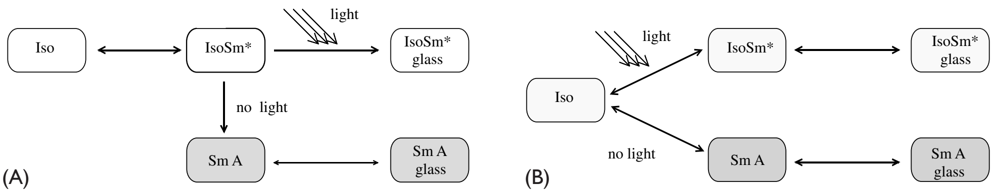

FIG. 5.25 Scheme of phase transitions in darkness and under illumination in chiral photochromic copolymers (A) SK8 and SK16 and (B) KW40 and KM45.

mers under discussion (Figure 5.5), the difference in mesomorphic behavior is especially pronounced within the intermediate range of copolymer compositions, corresponding to the metastable formation of the IsoSm* phase. In that range, the unpolarized light illumination can even switch the sequence of mesophases for the copolymer towards the formation of the IsoSm* phase or prevent some phase transitions.[97] The phenomenon of the light-controlled phase transitions (the LCPT effect) has been observed to date for at least four copolymers (the corresponding schemes of phase transformations in darkness and under light illumination are shown in Figure 5.25). To be specific, for SK8 and SK16, light illumination forbids the TGB A* → Sm A transition at 29°C on cooling, and for KW40 and KM45, it switches the phase sequence from Iso → Sm A to Iso → TGB A*. Once the phase is formed and frozen in glass at ambient temperature, it keeps the acquired structure (either transparent, IsoSm*, or turbid, Sm A) for years with no visible changes. Figure 5.26 illustrates the optical appearance of an LCPT copolymer film cooled down to room temperature either in darkness or under illumination with visible light. As seen from the scan, a turbid, birefringent multidomain Sm A texture is formed in the shadow area, but the illuminated spot acquires a transparent, optically isotropic IsoSm* structure (the short-pitch TGB A* phase).

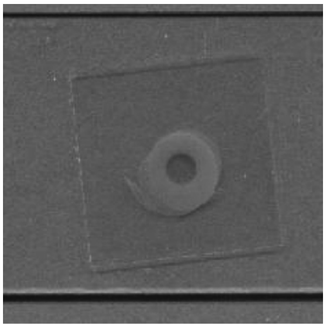

FIG. 5.26 Polymer film (SK16, ~23 μm) cooled from 70°C to ambient temperature at 0.5 K/min. The central spot was illuminated by a microscope lamp (nonpolarized), whereas the outside ring was not illuminated.

The two phase states of the same copolymer at the same temperature can be distinguished not only by their optical properties but also by X ray scattering[97] and dielectric relaxation measurements.[62] It is also worth noticing that the phase behavior of the polymers can be switched not only by nonfiltered white light of low intensity (e.g., from a desk lamp with power density 11 W/cm^2 within the wavelength range 350 to 2000 nm), but also selectively by blue-green light ($400 < \lambda < 500$ nm) with power density as low as 0.3 W/cm^2. That wavelength range corresponds to band **C** in the absorption spectra (Figure 5.8), and the same light causes the light-induced birefringence (Figure 5.11).

The LCPT effect originates undoubtedly from a change in the proportion of *cis*- and *trans*-isomers of azobenzene chromophores in the polymer film. It is still not clear, however, which of those isomers is more favorable for the formation of the IsoSm* structure and which prefers the straight Sm A type of packing. We found it reasonable to first suggest, that illumination within the n-π^* band suppresses *cis*-isomers completely and that the TGB A* structure cannot transform to the Sm A phase under illumination because of the excess of *trans*-configured azobenzene fragments, which would possess higher helical twisting power and "frustrate" the uniform smectic structure. That suggestion can be supported with our early observations[98] that the rod-like *trans*-isomer of a chiral low molar mass dye induces higher spontaneous polarization in the Sm C matrix than the banana-shaped *cis*-form does. Also, a ~3-μm-thick SK8 film cast from UV-irradiated solution (the *cis*-film) evidently forms Sm A phase, in contrast to the mostly *trans*-film cast from virgin solution.

On the other hand, as mentioned in Section 5.3, the *trans*-isomer also absorbs within band C, especially in the condensed state of the copolymer, so that illumination with blue-green light creates not a pure *trans*-film but a new steady-state proportion of both isomers. Moreover, UV irradiation of the Sm A film of SK8 has been reported to transform it back to the IsoSm* phase.[77] Therefore, the *cis*-isomers seem to be preferred for the formation of the TGB A* phase.

Whatever the explanation, the LCPT effect has been used successfully for photorecording purposes (a primitive setup for LCPT recording is shown in Figure 5.27). Actually, if a copolymer film is being cooled slowly from above the transition point and illuminated simultaneously through a mask, the Sm A phase forms in a shadow area under the mask. It scatters incident light strongly and appears white. At the same time, the cooling under illumination ends up with the short-pitch TGB A* (IsoSm*) phase. In other words, the written image is realized as a negative Sm A image on the IsoSm* background.

There are, then, three possibilities for reading out the recorded image. First, the image can be viewed in the scattering mode, if observed in the daylight or in standard illumination; it appears then as a white graph on the colorless background. This is illustrated in Figure 5.28A, where the name of one of this chapter's authors is recorded. The image has already been kept for three years at ambient temperature and shows no visible changes. Second, the image can be read out in the transmission (dia) mode when looking through

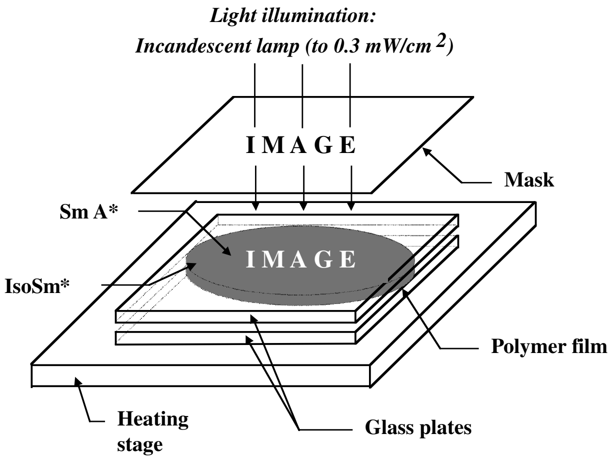

FIG. 5.27 Sketch of the photorecording setup.

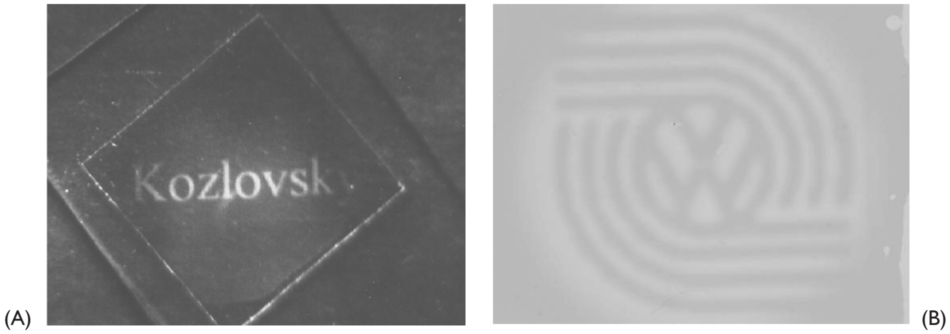

FIG. 5.28 Examples of LCPT-recorded images in a ~ 10-µm-thick SK8 film, observed in (A) the scattering mode and (B) the transmission mode.

the copolymer film; and appears then as a dark graph on the transparent background, as illustrated Figure 5.28B. We should emphasize here that no polarized light is necessary for either LCPT recording or reading of the image. Third, if crossed polarizers are used, the image can be read out as a white graph on the black background.

In contrast to photoinduced birefringence, the mesophase patterns in Figure 5.28 cannot be erased by light irradiation with UV light or with circularly polarized visible light, and only heating above the transition temperature erases the pattern. After such a thermal treatment, a new image can be written in the same film, up to 10 cycles of LCPT recording have been tested with a 10-µm-thick SK8 film without any loss in image quality.

To summarize, the LCPT effect allows a novel recording technique to be implemented. The technique is very simple to realize and allows for recording large-area images using nonpolarized light of low intensity.

5.7 CONCLUSIONS

The chiral side chain polymers derived from asymmetric esters of terephthalic acid and hydroquinone can form (in a broad temperature range, including ambient temperature) an unusual mesophase (the "isotropic smectic" phase, IsoSm*) characterized by high transparency and optical isotropy within the visible wavelength range, combined with a hidden layered smectic ordering and some elements of helical superstructure at shorter dimensions of 10 to 250 nm. The short-pitch TGB A* model seems to be the most adequate for the mesophase structure.

If functionalized with an azobenzene chromophore, the resulting copolymers also form the IsoSm* phase in a broad range of compositions. They show photochromism and photoinduced birefringence typical of azo dye LC copolymers, but they differ from the latter by their spontaneous formation of transparent, optically isotropic films, thus allowing for easy production of thick (up to 30 μm) photoactive layers. On the other hand, as compared with amorphous azobenzene-containing polymers, our copolymers possess some hidden liquid-crystalline ordering, which allows "imprinting" of photoinduced orientation of chromophores into the mesogenic matrix and/or main chain conformation during phase formation. Such imprinting can occur either on cooling or isothermally (in the case of kinetically governed transitions) and results in larger values of photoinduced birefringence and its higher stability.

Birefringence can be induced in optically isotropic photochromic IsoSm* copolymers by UV illumination and/or by visible light within the blue-green wavelength range of 400 to 500 nm. The latter is rather stable and shows no saturation up to several hours of illumination, whereas the birefringence induced by polarized UV light (300 to 400 nm) within the first few seconds disappears with further illumination. On the other hand, pretreatment with UV light increases substantially the sensitivity of the copolymer to the next photorecording within the blue-green range. Moreover, hidden UV images can be written by UV irradiation through a mask, and the visible images can be further developed by polarized uniform visible light.

Generally, photochromic IsoSm* films are considerably more sensitive to phase grating recording (created, e.g., by two laser beams of opposite circular polarization) than to intensity grating recording (with linearly polarized light). The gratings can be stable (for several months) or unstable (disappearing in few minutes) depending on the laser beam intensity, film pretreatment, and type of grating. Stable gratings can be erased with UV or circular light irradiation, or by heating the film above the phase transition point.

The most remarkable feature of the reported chiral azo dye copolymers, however, is the possibility of controling their phase transitions by light illumination. This capability is observed for the copolymer compositions within the range of metastable IsoSm* phase formation, and it has been applied for the novel photorecording technique, LCPT (light-controlled phase transition) recording. The recording is carried out with unpolarized visible light of low intensity, and the images are recorded as Sm A scattering patterns on the IsoSm* background. They can be easily read out with nonpolarized light, both in the scattering mode and in the transmission (dia) mode.

ACKNOWLEDGMENTS

This work was been supported by the Volkswagen Foundation (Project I 47 741), Deutsche Forschungsgemeinschaft (Project Re 923/8-1), and Russian Funds for Basic Research (Grant No. 01-02-16287). We are grateful to K. Yoshino and M. Ozaki (Department of Electronic Engineering, Osaka University, Japan), V. Lazarev (Institute of Crystallography, Russian Academy of Sciences, Moscow, Russia), and G. Gipparrone, N. Scaramuzza, and M. de Santo (Dipartimento di Fisica, Universitá della Calabria, Rende (Cs), Italy) for their participation in our experiments.

REFERENCES

1. McArdle, C. B. Ed. *Applied Photochromic Polymer Systems*. New York: Blackie & Son, Ltd. (1992).
2. Shibaev, V. P. Ed. *Polymers as Electro-optical and Photo-optical Media*. Berlin: Springer Verlag (1996).
3. Blinov, L. M. Photoinduced molecular reorientation in polymers, Langmuir-Blodgett films and liquid crystals. *J. Nonlin. Opt. Phys. Mater.* **5**, 165 (1996).
4. Todorov, T., Nikolova, L., and Tomova, N. Polarization holography. 1: A new high-efficiency organic material with reversible photoinduced birefringence. *Appl. Opt.* **23**, 4309 (1984).
5. Ivanov, M., Todorov, T., Nikolova, L., Tomova, N., and Dragostinova, V. Photoinduced changes in the refractive index of azo-dye/polyme systems. *Appl. Phys. Lett.* **66**, 2174 (1995).
6. Havinga, E. E., and van Pelt, P. Electrochromism of substituted polyalkenes in polymer matrixes; influence of chain length on charge transfer. *Ber. Bunsenges. Phys. Chem.* **83**, 816 (1979).
7. Blinov, L. M., Barnik, M. I., Weyrauch, T., Palto, S. A., Tevosov, A. A., and Haase, W. Photoassisted poling of polymer materials studies by stark spectroscopy (electroabsorption) technique. *Chem. Phys. Lett.* **231**, 246 (1994).
8. Barnik, M. I., Blinov, L. M., Weyrauch, T., Palto, S. A., Tevosov, A. A., and Haase, W. Stark spectroscopy as a tool for the characterization of poled polymers for nonlinear optics. In: G. A. Lindsay, K. O. Singer, Eds. *Polymmers for Second-Order Nonlinear Optics*, 288 (1995).
9. Natansohn, A., Rochon, P., Gosselin, J., and Xie, S. Azo polymers for reversible optical storage. 1. Poly[4′-[[2-(acryloyloxy)ethyl]ethylamino]-4-nitroazobenzene]. *Macromolecules* **25**, 2268 (1992).
10. Ho, M.-S., Natansohn, A., and Rochon, P. Azo polymers for reversible optical storage. 9. Cololymmers containing two types of azobenzene side groups. *Macromolecules* **29**, 44 (1996).
11. Natansohn, A., Rochon, P., Meng, X., Barrett, C., Buffeteau, T., Bonenfant, S., and Pézolet, M. Molecular addressing? Selective photoinduced cooperative motion of polar ester groups in copolymers containing azobenzene groups. *Macromolecules* **31**, 1155 (1998).
12. Hvilsted, S., Andruzzi, F., Kulinna, C., Siesler, H. W., and Ramanujam, P. S. Novel side-chain liquid crystalline polyester architecture for reversible optical storage. *Macromolecules* **28**, 2172 (1995).
13. Rasmussen, P. H., Ramanujam, P. S., Hvilsted, S., and Berg, R. H. A remarkably efficient azobenzene peptide for holographic information storage. *J. Am. Chem. Soc.* **121**, 4738 (1999).
14. Rasmussen, P. H., Ramanujam, P. S., Hvilsted, S., and Berg, R. H. Accelerated Optical Holographic Recording Using Bis-DNO. *Tetrahedron Lett.* **40**, 5953 (1999).
15. Si, J., Mitsui, T., Ye, P., Li, Z., Shen, Y., and Hirao, K. Optical storage in an azobenzene-polyimide film with high glass transition temperature. *Opt. Commun.* **147**, 313 (1998).
16. Fukuda, T., Matsuda, H., Shiraga, T., Kimura, T., Kato, M., Wiswanathan, N. K., Kumar, J., and Tripathy, S. K. Photofabrication of surface relief grating on films of azobenzene polymer with different dye functionalization. *Macromolecules* **33**, 4220 (2000).

17. Ringsdorf, H., Schmidt, H.-W., Baur, G., Kiefer, R., and Windscheid, F. Orientational ordering of dyes in the glassy state of liquid-crystalline side group polymers. *Liquid Crystals* **4**, 319 (1986).
18. Okazaki, S., Uto, S., Ozaki, M., and Yoshino, K. Guest-host electro-optic switching in spin-coated polymer ferroelectric liquid crystal film. *Appl. Phys. Lett.* **71**, 3373 (1997).
19. Jakob, E., Wolarz, E., Bialecka-Florjanczyk, E., Bauman, D., and Haase, W. Dielectric relaxation in a mixture of a side chain liquid crystalline polymer and a low molecular mass Azo Dye. *Mol. Cryst. Liq. Cryst.* **258**, 253 (1995).
20. Corvazier, L., and Zhao, Y. Induction of liquid crystal oreintation through azobenzene-containing polymer networks. *Macromolecules* **32**, 3195 (1999).
21. Zhao, Y., Chénard, Y., and Paiement, N. Liquid crystalline anisotropic gels based on azobenzene-containing networks. *Macromolecules* **33**, 1049 (2000).
22. Kurihara, S., Sakamoto, A., and Nonaka, T. Fast photochemical switching of a liquid-crystalline polymer network containing azobenzene molecules. *Macromolecules* **31**, 4648 (1998).
23. Kurihara, S., Sakamoto, A., Yoneyama, D., and Nonaka, T. Photochemical switching behavior of liquid crystalline polymer networks containing azobenzene molecules. *Macromolecules* **32**, 6493 (1999).
24. Kurihara, S., Matsumoto, K., and Nonaka, T. Optical shutter driven photochemically from anisotropic polymer network containing liquid crystalline and azobenzene molecules. *J. Appl. Phys. Lett.* **73**, 160 (1998).
25. Yamane, H., Kikuchi, H., and Kajiyama, T. Laser-addressing rewritable optical information storage of (liquid crystalline side chain copylymer/liquid crystals/photo-responsive molecule) ternary composite systems. *Polymer* **40**, 4777 (1999).
26. Wu, Y., Demachi, Y., Tsutsumi, O., Kanazawa, A., Shiono, T., and Ikeda, T. Photoinduced alignment of polymer liquid crystals containing azobenzene moieties in the side chain. 1. Effect of light intensity on alignment behavior. *Macromolecules* **31**, 349 (1998).
27. Wu, Y., Kanazawa, A., Shiono, T., Ikeda, T., and Zhang, Q. Photoinduced alignment of polymer liquid crystals containing azobenzene moieties in the side chain. 4. Dynamic study of the alignment process. *Polymer* **40**, 4787 (1999).
28. Wu, Y., Mamiya, J.-I., Kanazawa, A., Shiono, T., Ikeda, T., Nagase, Y., and Zhang, Q. Photoinduced alignment of polymer liquid crystals containing azobenzene moieties in the side chain. 6. Biaxiality and three-dimensional reorientation. *Macromolecules* **32**, 8829 (1999).
29. Eich, M., Wendorff, J. H., Reck, B., and HRingsdorf, H. Reversible digital and holographic optical storage in polymeric liquid crystals. *Makromol. Chem., Rapid Commun.* **8**, 59 (1987).
30. Eich, M. and Wendorff, J. H. Erasible holograms in polymeric liquid crystals. *Makromol. Chem. Rapid Commun.* **8**, 574 (1987).
31. Wendorff, J. H., and Eich, M. Nonlinear optical phenomena in liquid crystalline side chain polymers. *Mol. Cryst. Liq. Cryst.* **169**, 133 (1989).
32. Anderle, K. and Wendorff, J. H. Holographic recording using liquid crystalline side chain polymers. *Mol. Cryst. Liq. Cryst.* **243**, 51 (1994).
33. Ringsdorf, H., Urban, C., Knoll, W. and Savodny, P. Photoreactive chiral liquid-crystalline side-group copolymers containing azobenzene mesogens. *Makromol. Chem.* **193**, 1235 (1992).
34. Sawodny, M., Schmidt, A., Stamm, M., Knoll, W., Urban, C., and Ringsdorf, H. Langmuir-Blodgett-Luhn multilayer assemblies of liquid-crystalline azo-dye side chain homo- and copolymers. *Thin Solid Films* **210/211**, 500 (1992).
35. Shibaev, V. P., Kostromin, S. G., and Ivanov, S. A. Photoregulation of the optical properties of comb-shape polymers with mesogenic side groups and the problems of data recording. *Polym. Sci.* **39**, 118 (1997).
36. Kostromin, S. G., Shibaev, V. P., Geßner, U., Cackovic, H., and Springer, J. Oligoacrylates with cyanobiphenyl mesogenic groups. *Vysokomol. Soed. A* **38**, (1996).
37. Shibaev, V. P. Some new physico-chemical aspects of side chain liquid crystal polymers. *Mol. Cryst. Liq. Cryst.* **243**, 201 (1994).
38. Stumpe, J., Fischer, T., Ziegler, A., Geue, T., Menzel, H. Photoorientation in LB multilayers

of thermotropic polymers. *Mol. Cryst. Liq. Cryst.* **299**, 245 (1997).

39. Fisher, T., Läsker, L., Czapla, S., Rübner, J., and Stumpe, J. Interdependence of photoorientation and thermotropic self-organization in photochromic liquid crystalline polymers. *Mol. Cryst. Liq. Cryst.* **298**, 213 (1997).
40. Fischer, T., Läsker, L., Rutloh, M., Czapla, S., and Stumpe, J. Competition of self-organization and photo-orientation in liquid crystalline polymers. *Mol. Cryst. Liq. Cryst.* **299**, 293 (1997).
41. Sekkat, Z., Wood, J., Knoll, W., Volksen, W., Miller, R. D., and Knoesen, A. Light-induced orientation in azo-polyimide polymers 325°C below the glass transition temperature. *J. Opt. Soc. Am. B* **14**, 829 (1997).
42. Sekkat, Z., and Knoll, W.Photoreactive organic thin films in the light of bound electromagnetic waves. In: D. Neckers, D. Volman, and G. Von Buenau, Eds. *Adv. in Photochemistry* **22**, 117 (1997).
43. Sekkat, Z., and Dumont, M. Poling of azo dye doped polymerc films at room temperature. *Appl. Phys. B* **54**, 486 (1992).
44. Sekkat, Z., Aust, E. F., and Knoll, W. Photo-Induced Poling of Polar Azo dyes in Polymer films. In: G. Lindsay and K. Singer, Eds. *Polymers for Second-Order Nonlinear Optics*, *ACS Symp. Ser.* **601**, Ch. 19, 1995.
45. Blinov, L. M., Palto, S. P., Tevosov, A. A., Barnik, M. I., Weyrauch, Th., and Haase, W. Electrically and photoelectrically poled polymers for nonlinear optics: Chromophores' polar order and its relaxation studied by electroabsorption. *Mol. Mater.* **5**, 311 (1995).
46. Bobrovsky, A., Boiko, N., and Shibaev, V. Photo-optical properties of new combined chiral photochromic liquid crystalline copolymers. *Liquid Crystals* **25**, 393 (1998).
47. Bobrovsky, A., Boiko, N., and Shibaev, V., A new type of multifunctional materials based on dual photochromism of ternary photochromic liquid crystalline copolymers for optical data recording and storage. *J. Mater. Chem.* **10**, 1075 (2000).
48. Petri, A., Kummer, S., Anneser, H., Feiner, F., and Bräuchle, C. Photoinduced reorientation of cholesteric liquid crystalline polysiloxanes and applications in optical information storge and second harmonic generation. *Ber. Bunsenges. Phys. Chem.* **97**, 1281 (1993).
49. Hayashi, T., Kawakami, H., Doke, Y., Tsuchida, A., Onogi, Y., and Yamamoto, M. Photoinduced phase transition of side chain liquid crystalline copolymers with photochromic group. *Eur. Polym. J.* **31**, 23 (1995).
50. Ikeda, T., Horiuchi, S., Karanjit, D. B., Kurihara, S., and Tazuke, S. Photochemically induced isothermal phase transition in polymer liquid crystals with mesogenic phenyl benzoate side chains. 1. Calorimetric studies and order parameters. *Macromolecules* **23**, 36 (1990).
51. Kanazawa, A., Hirano, S., Shushido, A., Hasegawa, M., Tsutsumi, O., Shiono, T., Ikeda, T., Nagase, Y., Akiyama, E., and Takamura, Y. Photochemical phase transition behavior of polymer azobenzene liquid crystals with flexible siloxane units as a side-chain spece. *Liquid Crystals* **23**, 293 (1997).
52. Tsu-tsumi, O., Kitsunai, T., Kanazawa, A., Shiono, T., and Ikeda, T. Photochemical phase transition behavior of polymer azobenzene liquid crystals with electron-donating and –accepting substituents at the 4,4′-positions. *Macromolecules* **31**, 355 (1998).
53. Gu, J., Liang, B., Liu, L., Tian, Y., Chen, Y., Lu, B., and Lu, Z. Photoinduced properties of liquid crystalline azobenzene polymer in Langmuir-Blodgett films investigated by surface plasmon resonance. *Thin Solid Films* **327–329**, 427 (1998).
54. Tian, Y., Ren, Y., Sun, R., Zhao, Y., Tang, X., Huang, X., and Xi, S. Synthesis of a series of chiral coplymers with azo groups and investigations of reversible liquid crystalline alignment induced by the LB films of these materials. *Liquid Crystals* **22**, 177 (1997).
55. Fischer, T., Menzel, H., and Stumpe, J. Photo-reorientation of azobenzene side grops of thermotropic 'hairy rod' polyglutamate in LB multilayers. *Supramol. Sci.* **4**, 543 (1997).
56. Andruzzi, L., Altomare, A., Ciardelli, F., Solaro, R., Hvilsted, S., and Ramanujam, P. S. Holographic gratings in azobenzene side-chain polymethacrylates. *Macromolecules* **32**, 448 (1999).
57. Labarthet, F. L., Freiberg, S., Pellerin, C., Pézolet, M., Natansohn, A., and Rochon, P. Spectroscopic and optical characterization of a series of azobenzene-containing side-chain liquid crystalline polymers. *Macromolecules* **33**, 6815 (2000).

58. Si, J., Mitsui, T., Ye, P., Li, Z., Shen, Y., and Hirao, K. Optical storage in an azobenzene-polyimide film with high glass transition temperature. *Opt. Commun.* **147**, 313 (1998).
59. Kulinna, C., Hvilsted, S., Hendann, C., W-Siesler, H., Ramanujam, P. S. Selectively deuterated liquid crystalline cyanobenzene side-chain polyesters. 3. Investigations of laser-induced segmental mobility by Fourier Transform Infrared Spectroscopy. *Macromolecules* **31**, 2141 (1998).
60. Bata, L., Fodor-Csorba, K., Szabon, J., Kozlovsky, M. V., and Holly, S. A chiral side-chain polymer with layered structure. *Ferroelectrics* **122**, 149 (1991).
61. Kozlovsky, M. V., Fodor-Csorba, K., Bata, L., Shibaev, V. P. Chiral smectic side-chain copolymers. 1. Synthesis and phase behavior. *Eur. Polym. J.* **28**, 901 (1992).
62. Kilian, D., Kozlovsky, M. V., and Haase, W. Dielectric measurements on the 'isotropic smectic phase' of dyed side chain polymers. *Liquid Crystals* **26**, 705 (1999).
63. Kozlovsky, M. V., Haase, W., Kuball, H.-G. Influence of chirality on mesophase state of side chain polymers with phenyl benzoate mesogenic groups. In: *6th European Conference on Liquid Crystals*; March 25–30, 2001, Halle (Saale), Germany. Abstracts, 5-P14.
64. Demikhov, E., Kozlovsky, M. V. Amorphous chiral smectic A phase of side chain copolymers. *Liquid Crystals* **18**, 911 (1995).
65. Vill, V. *LiqCryst 3.3. Database of Liquid Crystalline Polymers*. Hamburg: LCI Publischer GmbH (1999).
66. Renn, S. R., Lubensky, T. C. Abrikosov dislocation lattice in a model of the cholesteric—to—smectic-A transition. *Phys. Rev. A* **38**, 2132 (1988)
67. Renn, S. R., Lubensky, T. C. Existence of a Sm-C grain boundary phase at the chiral NAC point. *Mol. Cryst. Liq. Cryst.* **209**, 349 (1991).
68. Goodby, J. W., Waugh, M. A., Stein, S. M., Chin, E., Pindak, R., and Patel, J. S. A new molecular ordering in helical liquid crystals. *J. Am. Chem. Soc.*, **111**, 8119 (1989)
69. Navaliles, L., Barois, P., Nguyen, H. T. X-ray measurement of the twist grain boundary angle in the liquid crystal analog of the Abrikosox phase. *Phys. Rev. Lett.* **71**, 545 (1993).
70. Goodby, J. W. Twist grain boundary (TGB) phases. In: D. M. P. Mingos Ed. *Liquid crystals II. Structure and bonding*, Vol. 95, New York: Springer Verlag, 83 (1999).
71. Kitzerow, H.-G. Twist Grain Boundary Phases. In: C. Bahr, H. Kitzerow Eds. *Chirality in liquid crystals*. New York: Springer Verlag, 297 (2000).
72. Dierking, I., Lagerwall, S. T. A review of textures of the TGBA* phase under different anchoring geometries. *Liquid Crystals*, **26**, 83 (1999)
73. Kozlovsky, M. V., Haase, W., Stakhanov, A., and Shibaev, V. P. Chiral smectic side-chain copolymemrs. 3. Copolymers containing a diazo chromophore. *Mol. Cryst. Liq. Cryst.*, **321**, 177 (1998).
74. Kozlovsky, M. V., Meier, J. G., and Stumpe, J. Chiral side chain copolymers. 4. Kinetics of the phase transition from conventional isotropic liquid to the TGB-like "isotropic smectic" state. *Macromol. Chem. Phys.*, **201**, 2377 (2000).
75. Blinov, L. M., Barberi, R., Kozlovsky, M. V., Lazarev, V. V., and Santo, M. P. Optical anisotropy and four possible orientations of a nematic liquid crystal on the same film of a photochromic chiral smectic polymer. *J. Nonlinear Opt. Phys.Mat.*, **9**, 1 (2000).
76. Blinov, L. M., Kozlovsky, M. V., Ozaki, M., Skarp, K., and Yoshino, K. *J. Appl. Phys.* **84**, 3860 (1998).
77. Blinov, L. M., Kozlovsky, M. V., and Gipparone, G. Photochromism and holographic grating recording on a chiral side-chain polymer containing azobenzene chromophores. *Chem. Phys.*, **245**, 473 (1999).
78. Blinov, L. M., Gipparone, G., Kozlovsky, M. V., Lazarev, V. V., Scaramuzza, N. Holographic "development' of a hidden UV image recorded on a liquid crystalline polymer. *Optics Commun.* **73**, 137 (2000).
79. Blinov, L. M., Kozlovsky, M. V., Ozaki, M., Yoshino, K. Effect of the trans-cis isomerization of a chiral azo-dye on the dye induced ferroelectricity in an achiral liquid crystal. *Mol. Mat.* **6**, 235 (1996)
80. Blinov, L. M., Barberi, R., Cipparrone, G., Kozlovsky, M. V., Lazarev, V. V., Ozaki, M., de Santo, M. P., Scaramuzza, N., and Yoshino, K. Reversible UV Image Recording on a photochromic side chain liquid crystalline polymer. *Mol. Cryst. Liq. Cryst.* **355**, 359–380 (2001).

81. Kozlovsky, M. V., and Lazarev, V. V. The photoinduced birefringence in thick films of chiral azodye copolymers (submitted to *Macromol. Chem. Phys.*)
82. Han, M., Morino, S., and Ichimura, K. Factors affecting in-plane and out-of-plane photo-orientation of azobenzene side chains attached to liquid crtstalline polymers induced by irradiation with linearly polarized light. *Macromolecules* **33**, 6360 (2000).
83. Buse, K., Adibili, A., and Psaltis, D. Non-volatile holographic storage in doubly doped lithium niobate crystals. *Nature* **393**, 665 (1998).
84. Gipparone, G., Mazzulla, A., Kozlovsky, M. V., Palto, S. P., Yudin, S. G., and Blinov, L. M. Polarization gratings in photosensitive Langmuir-Blodogett films and chiral liquid crystalline polymers. *Mol. Mat.* **12**, 359 (2000).
85. Kozlovsky, M. V., and Haase, W. Photorecording in the "isotropic smectic phase" of dyed side-chain polymers. *Macromol. Symp.* **137**, 47 (1999).
86. Petrov, M. P., Stepanov, S. I., Khomenko, A. V. *Photorefractive Crystals in Coherent Optical Systems*. Berlin: Springer, (1991).
87. Blanche, P.-A., Lemaire, Ph. C., Maertens, C., Dubois, P., and Jérôme, R. Polarization holography reveals the nature of the grating in polymers containing azo-dye. *Opt. Commun.*, **185**, 1 (2000)
88. Blinov, L. M., Cipparrone, G., and Palto, S. P. Phase grating recording on photosensitive Langmuir-Blodgett films. *Int. J. Nonlin. Opt. Phys.*, **7**, 369 (1998).
89. Couture, J. J. A. Polarization holographic characterization of organic azo dyes/poly(vinyl alcohol) filmms for real time applications. *Appl. Optics*, **30,** 2858 (1991).
90. Dydyusha, A. G., Kozenkov, V. M., Marusii, T. Ya., Reznikov, Yu. A., Reshetnyak, V. Yu., and Khizhnyak, A. I. Light induced planar orientation of nematic liquid crystals on photo-anisotropic surface without a microrelief. *Ukr. Fiz. Zh.* **36**, 1059 (1991).
91 Schadt, M., Schmit, K., Kozenkov, V., and Chigrinov, V. Surface-induced parallel alignment of liquid crystals by linearly polymerized photopolymers. *Jpn. J. Appl. Phys.* **31**, 2155 (1992).
92. Gibbons, W., Shannon, P., Shao-Tang Sun, and Swetlin, B., Surface mediated alignment of nematic liquid crystals with polarized laser light. *Nature* **351**, 49 (1991).
93. Schadt, M., Seiberle, and Schuster, A. Optical patterning of multidomain liquid-crystal displays with wide viewing angles. *Nature* **381**, 212 (1996).
94. Perny, S., Le Barny, P., Delaire, J., Buffeteau, T., Sourisseau, C., Dozov, I., Forget, S., and Martinot-Lagarde, P. Holoinduced orientation in poly(vinylcinnamate) and poly(7-methacryloyloxycoumarin) thin films and the consequences on liquid crystal alignment. *Liquid Crystals* **27**, 329 (2000).
95. Palto, S., Barberi, R., Iovane, M., Lazarev, V. V., and Blinov, L. M. Measurements of zenithal anchoring energy of nematics at the planar interface in hybrid cells. *Mol. Mat.* **12**, 277 (2000).
96. Yokoyama, H., and van Sprang, H. A. A novel method for determining the anchoring energy function at a nematic liquid crystal-wall interface from director distortions at high fields. *J. Appl. Phys.* **57,** 4520 (1985).
97. Kozlovsky, M. V., Shibaev, V. P., Stakhanov, A. I., Weyrauch, T., Haase, W., and Blinov, L. M. A new approach to photorecording based on hindering the TGB A* – Sm A* phase transition in photochromic chiral liquid crystalline polymers. *Liquid Crystals* **24**, 759 (1998).
98. Blinov, L. M., Kozlovsky, M. V., Nakayama, K., Ozaki, M., and Yoshino, K. Photochromism of azo-dyes and effect of liquid crystalline ordering on its efficiency and kinetics. *Japan. J. Appl. Phys.* **35**, 5405 (1996).